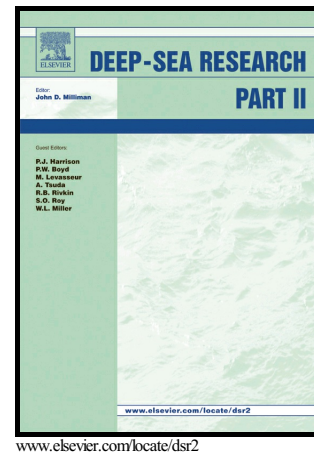


Author's Accepted Manuscript

Three decades of deep water mass investigation in the Weddell Sea (1984–2014): temporal variability and changes

Rodrigo Kerr, Tiago S. Dotto, Mauricio M. Mata, Hartmut H. Hellmer



PII: S0967-0645(17)30126-1
DOI: <https://doi.org/10.1016/j.dsr2.2017.12.002>
Reference: DSR114362

To appear in: *Deep-Sea Research Part II*

Received date: 12 April 2017
Revised date: 24 November 2017
Accepted date: 3 December 2017

Cite this article as: Rodrigo Kerr, Tiago S. Dotto, Mauricio M. Mata and Hartmut H. Hellmer, Three decades of deep water mass investigation in the Weddell Sea (1984–2014): temporal variability and changes, *Deep-Sea Research Part II*, <https://doi.org/10.1016/j.dsr2.2017.12.002>

This is a PDF file of an unedited manuscript that has been accepted for publication. As a service to our customers we are providing this early version of the manuscript. The manuscript will undergo copyediting, typesetting, and review of the resulting galley proof before it is published in its final citable form. Please note that during the production process errors may be discovered which could affect the content, and all legal disclaimers that apply to the journal pertain.

Three decades of deep water mass investigation in the Weddell Sea (1984–2014): temporal variability and changes

Rodrigo Kerr^{1,2,*}, Tiago S. Dotto^{1,2,*a}, Mauricio M. Mata^{1,2}, and Hartmut H. Hellmer³

¹Laboratório de Estudos dos Oceanos e Clima, Instituto de Oceanografia, Universidade Federal do Rio Grande – FURG, Rio Grande, RS, 96203-900, Brazil.

²Grupo de Estudos do Oceano Austral e Gelo Marinho, Instituto Nacional de Ciência e Tecnologia da Criosfera (INCT-CRIOSFERA), Rio Grande, 96203-900, RS, Brazil.

³Stiftung Alfred-Wegener-Institut für Polar- und Meeresforschung in der Helmholtz-Gemeinschaft, Bussestraße 24, 27570 Bremerhaven, Germany.

*These authors contributed equally to this work.

^aNow at: Ocean and Earth Science, University of Southampton, National Oceanography Centre, Southampton, UK.

*Corresponding author:

Address: Instituto de Oceanografia, Universidade Federal do Rio Grande – FURG, Avenida Itália km 8 s/n°, Campus Carreiros, Rio Grande – RS, Brazil, 96203–900

E-mail: rodrigokerr@furg.br; tiagosdotto@gmail.com

Phone number: +55 53 3233-6858

Running title: Weddell deep waters variability

Highlights

- Shifts in Weddell Sea Bottom Water (WSBW) properties towards less dense varieties likely equate to less WSBW being produced over time.
- The decline of WSBW volume ceased around 2005 and likely recovering after that.
- Dense Shelf Waters drive and modulate the recent WSBW variability.
- WSBW is composed by 71% of Warm Deep Water and 29% of Dense Shelf Waters.

Abstract

The role of Antarctic Bottom Water (AABW) in changing the ocean circulation and controlling climate variability is widely known. However, a comprehensive understanding of the relative contribution and variability of Antarctic regional deep water mass varieties that form AABW is still lacking. Using a high-quality dataset comprising three decades of observational shipboard surveys in the Weddell Sea (1984–2014), we updated the structure, composition and hydrographic properties variability of the Weddell Sea deep-layer, and quantified the contribution of the source waters composing Weddell Sea Bottom Water (WSBW) in its main formation zone. Shifts in WSBW hydrographic properties towards less dense varieties likely equate to less WSBW being produced over time. WSBW is primarily composed of $71\pm4\%$ of modified-Warm Deep Water (mWDW) and $29\pm4\%$ of Dense Shelf Waters, with the latter composed by \sim two-thirds ($19\pm2\%$) of High Salinity Shelf Water and \sim one-third ($10\pm6\%$) of Ice Shelf Water. Further, we show evidence that WSBW variability in the eastern Weddell Sea is driven by changes in the inflow of Dense Shelf Waters and bottom water from the Indian Sector of the Southern Ocean. This was observed through the rise of the WSBW contribution to the total mixture after 2005, following a twenty-year period (1984–2004) of decreasing contribution.

Key words: Deep Ocean, Antarctic Bottom Water, Dense Shelf Water, Southern Ocean.

1. Introduction

Several recent studies have debated about the causes and effects of Antarctic Bottom Water (AABW) variability and changes both in its source area and throughout the global ocean (e.g., Schmidtko et al. 2014; Azaneu et al., 2013; Purkey and Johnson, 2010, 2012, 2013). AABW is one of the major water mass of the lower limb of the global overturning circulation (e.g. Talley, 2013) and is composed of distinct regional dense water varieties sourced and/or modified around the Antarctic continent (e.g. Whitworth et al., 1998; Pardo et al., 2012). Its formation is driven by numerous coupled ocean-atmosphere-cryosphere processes taking place in the Southern Ocean (e.g., ocean-atmosphere heat fluxes, sea ice formation and melting, ocean-ice-shelf interaction, water mass mixing, ocean frontal instabilities, etc.). Briefly, those coupled processes increase the water mass density in the resulting mixture, which eventually leads to a dense plume overflow down the continental slope towards the deep ocean (Orsi et al., 1999; 2001; Ivanov et al., 2004; Nicholls et al., 2009).

Two distinct AABW formation processes have been previously described in the Weddell Sea (Fig. 1), the source region of the main AABW regional variety exported to the global ocean (e.g. Orsi et al., 2002; Kerr et al., 2012a; van Seville et al., 2013; Ferreira and Kerr, 2017). The first one was proposed by Foster and Carmack (1976a) after intensive studies in the Weddell Sea during the 1970s (e.g., Carmack, 1974; Carmack and Foster, 1975a, 1975b; Foster and Carmack, 1976b). It assumes that the mixing of dense High Salinity Shelf Water (HSSW) and modified-Warm Deep Water (mWDW; a mixture of Winter Water (WW) and Warm Deep Water (WDW)) at the continental shelf-break in the southern Weddell Sea forms the densest AABW regional variety: Weddell Sea Bottom Water (WSBW). As the dense WSBW follows the continental slope, it remixes with WDW resulting in the less dense variety of AABW in

the Weddell Sea: Weddell Sea Deep Water (WSDW). Recently, van Caspel et al. (2016) showed that the Larsen Ice Shelf region also plays a key role modulating the hydrographic properties and, consequently, the formation process of AABW varieties in the northwestern Weddell Sea (Gordon et al., 1993). The second process was introduced by Foldvik et al. (1985) and involves the mixture of WDW/mWDW and Ice Shelf Water (ISW)—a water mass with temperatures below surface freezing derived from the interaction of HSSW within the base of the ice-shelves in the southern Weddell Sea (Nicholls et al., 2001, 2004).

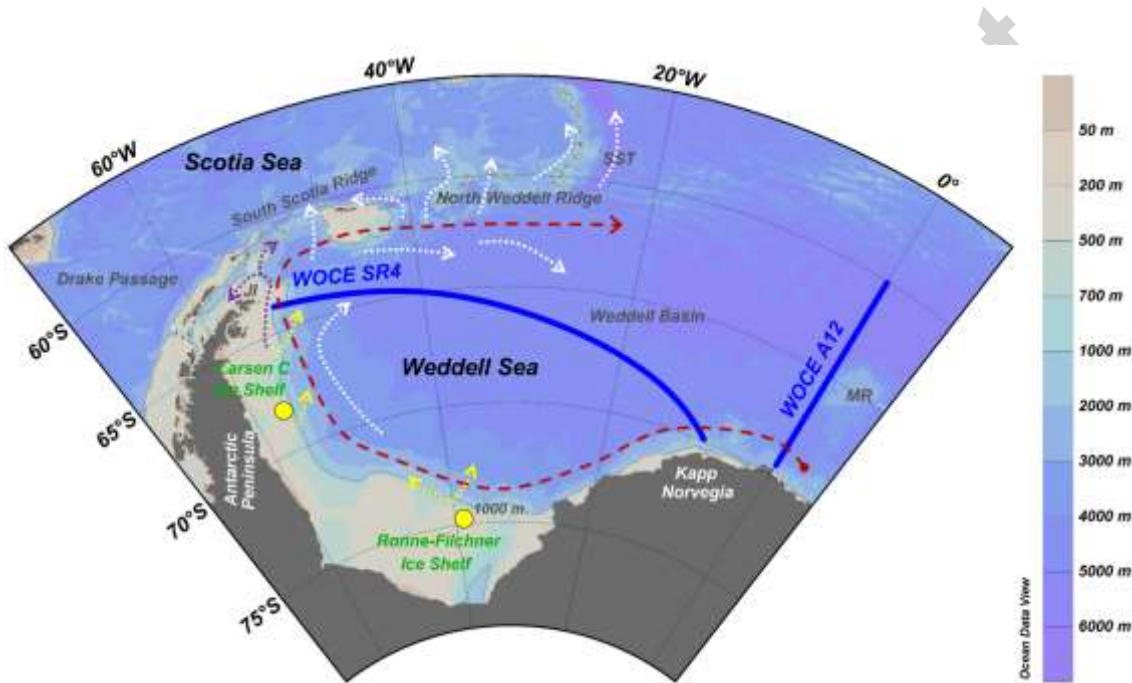


Figure 1. The study area in the Weddell Sea showing the location of the hydrographic sections (solid blue lines) across the Weddell Gyre (schematically indicated by the dashed red arrow) along the Greenwich Meridian (southern part of WOCE A12 repeat line) and across the Weddell Sea (WOCE SR4 repeat line) between Kapp Norvegia and Joinville Island (JI). The yellow dots mark the primary areas of AABW varieties formation, while the yellow dotted arrows schematically show sinking water masses along the continental slope. The dotted purple arrows indicate Dense Shelf Water living the northwestern Weddell Sea. The dotted white arrows depict deep and bottom water circulation and water masses exporting the Weddell Basin. This figure was sketched according to the studies of Gordon et al. (2001), von Gyldenfeldt et al. (2002), Naveira Garabato et al. (2002), Fahrbach et al. (2011), and Ferreira and Kerr (2017). See Table 1 for the sections occupation periods between 1984 and 2014. The bathymetry (m) is represented as a color scale bar at the right. MR = Maud Rise; SST = South Sandwich Trench. Bathymetry line of 1000 m is represented by the thin black line. (For interpretation of the references to color in this figure legend, the reader is referred to the web version of this article.)

Whitworth et al. (1998), through a detailed study of all Antarctic margins, proposed that WSBW can be formed by mixing of mWDW with HSSW or ISW depending if the east or west side of the basin considered, i.e., combining the AABW formation processes proposed by Foster and Carmack (1976a) and Foldvik et al. (1985). A detailed review of ice-ocean processes on the continental shelf of the southern Weddell Sea was further compiled by Nicholls et al. (2009), whereas Heywood et al. (2014) summarized the processes at the Antarctic continental shelf-break that are important for cross-slope exchanges of heat, freshwater, nutrients, and biota. In summary, despite the local ocean-, atmosphere- and cryosphere-related processes involved in the formation of AABW varieties in the Weddell Sea sub-regions, WSDW and WSBW in the deep Weddell Basin can be considered as a mixture of WW (i.e. a remnant of the deep winter mixed layer), WDW, HSSW and ISW. The first two water masses mix and are modified through the dynamic processes occurring in the Weddell Gyre regime (often referred to as mWDW), while the AABW shelf-components are regionally confined and modified through the coastal, air-sea and ice-land-sea processes occurring in the continental shelf regime.

Much less often, deep ocean convection in open ocean polynyas can directly form and modulate AABW varieties in the Southern Ocean (Gordon, 1978; Gordon, 2014). Although the recent appearance of this phenomenon in 2016 and 2017, this has not been observed with the dimensions and persistence of the Weddell Polynya since the events occurred in the 1970s (Comiso and Gordon, 1987; Gordon et al., 2007). This process, although more related to coastal polynyas, may occur in other important AABW formation regions outside the Weddell Sea as well (Ohshima et al., 2013; Kitade et al., 2014). It is also important to consider that AABW varieties sourced in the Weddell Sea and present in the easternmost part of the Weddell Basin are strongly

influenced by deep and bottom waters which originated to the East of the Weddell Sea (Meredith et al., 1999; 2000). This AABW variety enters the Weddell Gyre from the Indian Sector of the Southern Ocean, allowing further ventilation and densification of Weddell Sea AABW varieties within the gyre (Jullion et al., 2014).

AABW has a global and climate importance because it ventilates and renews the properties of the near-bottom layer of the global ocean (Schröder et al., 2002; Jacobs, 2004; Ferreira and Kerr, 2017). Considering the Weddell Sea regional AABW varieties, WSDW can enter the global ocean easier than WSBW (Naveira Garabato et al., 2002; Franco et al., 2007) because WSDW is less dense and thus not completely constrained within the Weddell Basin by the South Scotia Ridge (Gordon et al., 2001; Muench and Hellmer, 2002). Export of WSBW to the global ocean occurs through upward mixing with WSDW above or likely through outflows via deep passages (e.g., South Sandwich Trench; Fig. 1; Ferreira and Kerr, 2017).

Recently, Hellmer et al. (2016) performed a comprehensive review study based on field observations and modelling efforts of meteorology and oceanography of the Atlantic Sector of the Southern Ocean (i.e. Weddell-Enderby Basin). Those authors synthesized the Weddell Sea state-of-the-art knowledge regarding the interaction between the ocean and ice shelves, the physical processes related to water mass formation and changes, and marine chemistry issues regarding the associated storage of anthropogenic carbon in that region. Furthermore, as highlighted by Meredith et al. (2014), there is an essential need to identify and understand the AABW (and its regional varieties) time-varying formation and export processes, and the controls on properties and flows. For example, in the Australian Antarctic Sector Wijk and Rintoul (2014) have reported that the lightning of AABW layer cannot be explained by changes in formation rate alone, rather resulting from the contribution of less dense AABW

varieties. On the other hand, Azaneu et al. (2013) suggested that changes in formation rate may also have significant contribution to the contraction of AABW volumes in the Weddell-Enderby Basin. Thus, it is important to understand the causes of AABW properties, export and source-composition variability (e.g. Fahrbach et al. 2004; 2011), especially at its source zones, to assess how AABW evolves during time. This may potentially affect its significance for the global ocean overturning circulation and climate.

In this context, this study aims to investigate the temporal variability of the Weddell Sea deep water masses during the last three decades from 1984 to 2014. Taking advantage of an extensive dataset, we update the results regarding the temporal variability of the relative contribution of the deep water masses in the Weddell Sea previously reported by Kerr et al. (2009a). Those authors analyzed the Weddell Sea deep water mass structure between 1984 and 1998 and found a 20%-reduction in the WSBW contribution to the total mixture during that period. Moreover, the present analysis allows for a better understanding of the primary causes changing the WSBW layer and provides new insights to the scientific discussion about the causes of the Southern Ocean deep and bottom water variability and changes.

2. Data and Methods

2.1. Hydrographic section data

The potential temperature (θ) and practical salinity (S) were selected from two World Ocean Circulation Experiment (WOCE) hydrographic repeat sections in the Weddell Sea (Tab. 1; Fig. 1) as follows: (i) section WOCE A12 (also referred to as WOCE SR2 in the literature) along the Greenwich Meridian, with an irregular sampling period spanning from 1984 to 2014; and (ii) section WOCE SR4 between Joinville

Island and Kapp Norvegia, with an irregular sampling period spanning between 1989 and 2010. Section WOCE A12 was restricted here to latitudes higher than 60°S, whereas WOCE SR4 crossed the entire Weddell Sea (Fig. 1). Those sections were chosen because of their importance to: (i) the regional basin circulation (e.g., Klatt et al., 2005; Meredith et al., 2014), (ii) the export routes of deep and bottom waters (e.g., Naveira Garabato et al., 2002; Kerr et al., 2012a), and the representativeness for the entire Weddell Basin (e.g., Kerr et al., 2009a; Fahrbach et al., 2011; Jullion et al., 2014). Moreover, here we extend the period analyzed by Kerr et al. (2009a) to ~30 years taking advantage of the inclusion of five/two additional years at the Greenwich Meridian (WOCE A12) and in the inner Weddell Sea (WOCE SR4), respectively (Table 1). We also performed a novel mixing scheme approach (see Sect. 2.3) to quantify changes in the source waters of the WSBW.

Table 1. Overview of the hydrographic sections used in this study. Details of the observed data can be found in Whitworth and Nowlin (1987), Fahrbach et al. (2001, 2004, 2007, 2011), Fahrbach and De Baar (2010), Rohardt et al. (2011), van Heuven et al. (2011, 2014), Rohardt and Boebel (2015), and Driemel et al. (2017).

Expedition	Cruise Period (dd/mm/yyyy)	WOCE section
AJAX (leg 2)	16/01/1984 – 29/01/1984	A12
ANT-VIII/2	06/09/1989 – 31/10/1989	SR4
ANT-IX/2	16/11/1990 – 30/12/1990	SR4
ANT-X/4	21/05/1992 – 30/07/1992	A12
ANT-X7	03/12/1992 – 23/01/1993	SR4
ANT-XIII/4	17/03/1996 – 20/05/1996	A12 and SR4
ANT-XV/4	28/03/1998 – 23/05/1998	A12 and SR4*
ANT-XVI/2	09/01/1999 – 16/03/1999	A12
ANT-XVIII/3	05/12/2000 – 12/01/2001	A12
ANT-XX/2	24/11/2002 – 23/01/2003	A12
ANT-XXII/3	21/01/2005 – 06/04/2005	A12 and SR4
ANT-XXVII/2	28/11/2010 – 05/02/2011	A12 and SR4
ANT-XXIX/2	02/12/2012 – 14/01/2013	A12
PS89 (ANT-XXX/2)	02/12/2014 – 31/01/2015	A12

*During this year, the section WOCE SR4 was not completely surveyed.

The dataset used was downloaded through the World Ocean Database 2013 (WOD13; www.nodc.noaa.gov) and the Alfred Wegener Institute repository

(www.pangaea.de) websites. All observed θ and S data were sampled by high-accuracy CTDs and passed through strict data quality control (e.g., Johnson et al., 2013), eventually spurious data was manually removed from the compiled dataset. Five different CTD types have been used onboard R/V *Polarstern* from 1983 to present days. As the instruments have changed, so have the range, accuracy, stability, resolution, and response of the sensors. A detailed summary of the instruments' manufacturer specifications of the instruments as well as the periods they have been on duty is provided in Table 1 and Figure 1 of Driemel et al. (2017), respectively. For reference, the accuracy limits officially adopted for WOCE are also listed in Table 1 of Driemel et al. (2017). In general, the accuracy of θ , S , and pressure is better than $\pm 0.003^\circ\text{C}$, ± 0.003 and ± 2 dbar for the cruises, respectively (Fahrbach et al., 2011; van Heuven et al., 2014). Data for dissolved oxygen (DO) was obtained from discrete bottle samples before 2005 and after that by profiling CTD sensors, which were regularly calibrated against Winkler titrations, with a reported final accuracy of $4.5 \mu\text{mol kg}^{-1}$ (van Heuven et al., 2011). Other information regarding the quality, precision, and calibrations eventually applied to the θ , S , and DO dataset can be obtained through the references cited in the caption of Table 1.

In addition, we used an ancillary dataset obtained in the Indian Ocean Sector of the Southern Ocean to discuss the results found (see Section 4). Four repeat occupations along the section WOCE I6S at 30°E were obtained via the WOD13 for the years of 1993, 1996, 2006, and 2008. The same dataset was previously analyzed by Couldrey et al. (2013), where more specific details about the dataset can be found. For this dataset, the northern limit was restricted to 60°S and spurious data was manually removed.

2.2. Optimum Multiparameter (OMP) analysis

The OMP analysis package (Karstensen and Tomczak, 1999) has been used here to (i) estimate the vertical distribution, (ii) quantify the mixture, and (iii) elucidate about the temporal variability of the Weddell Sea deep water masses and the source waters of WSBW along to hydrographic sections across the Weddell Sea. The method was first introduced by Tomczak (1981) as an extension of the classical water mass analysis by means of temperature-salinity diagrams (Mamayev, 1975). Mackas et al. (1987), Tomczak and Large (1989), and Karstensen and Tomczak (1997, 1998) considerably improved the method allowing for more robust applications. Since then, the OMP analysis has been successfully applied throughout the global ocean to determine the relative water mass fractions of contribution on (i) regional (e.g., Huhn et al., 2008; Jenkins et al., 2014; García-Ibáñez et al., 2015; van Caspel et al., 2015; Dotto et al., 2016), (ii) ocean basin (e.g., Poole and Tomczak, 1999; Kerr et al., 2009a; Pardo et al., 2012; Santos et al., 2016; Ferreira and Kerr, 2017), and (iii) global (e.g., Johnson, 2008) scales. The method was also effectively used to distinguish water mass fractions of mixtures and eventual biases in Southern Ocean studies using numerical modeling and ocean reanalysis products (e.g., Kerr et al., 2009b, 2012b).

Briefly, the OMP analysis quantifies the relative fractions of a mixture (or contributions in % to the total mixture) of distinct source water types (SWT—parameter values that represent a water mass in its source region) by solving an over-determined system of linear mixing equations. The following parameters are considered to distinguish the water mass contributions: θ , S , and DO . Thus, the linear mixing equations can be expressed in matrix form as Eq. 1:

$$Gx - d = R \quad (1)$$

where G is the SWT matrix, which contains the parameter indices (i.e. θ , S , and DO) that represent each of the SWT ($i=1,\dots,3$); x is the relative contribution from each water sample; and the vectors d and R correspond to the observed dataset and the analysis residuals, respectively. The only restriction to the method is that the total contribution from all SWT considered in the mixing scheme must add to 100%. Negative SWT contributions are not allowed as there is no physical meaning to such numbers. It is also worth mentioning that the OMP analysis was applied in a region of AABW formation (see Section 2.3). Thus, the increase of one water mass in the mixture of a given year will necessarily mean that at least one other water mass will decrease its contribution to the total mixture to assure mass conservation.

OMP assumes that all the parameters have the same representativeness. However, this criterion is not often met because of the influence of environmental variability and the accuracy of the measurements. Thus, a weighted version of the G matrix was applied by including a diagonal matrix W , which has respective weights for each parameter ($j=\theta, S, DO$), to correct the external influences. According to Tomczak and Large (1989), the diagonal matrix W is obtained by Eq. 2:

$$W_j = \frac{\sigma_j^2}{\delta_{jmax}} \quad (2)$$

where σ_j^2 is the variance of each parameter among all SWT and δ_{jmax} is the maximum variance, among the water masses, associated with the same parameter in the source region. Here, we estimated our own parameter weights instead of arbitrarily define the values (see caption of Table 2). Mass conservation normally receive the highest weights found amongst the parameter weights. Mixing equations are weighted to optimize the use of hydrographic data, so the mass conservation residuals objectively indicate the

quality of the solution, which are normally assumed to be lower than 5–10% (e.g. Tomczak, 1999; Kerr et al. 2009a). Therefore, a low mass conservation residual indicates that the properties of the water sample are well represented by the SWT considered in the mixing scheme (Poole and Tomczak, 1999).

2.3. Deep water mixing schemes and source water types (SWT)

As the study region (i.e., the Weddell Sea) is also a source area of distinct AABW varieties, two mixing schemes have been considered here to tackle the proposed aims (Fig. 2). The first one (hereafter referred to as *Case A*) follows the same approach used by Kerr et al. (2009a), which aims to compute the fractions of mixture of the deep water masses that fill the Weddell Basin. In this sense, the following water masses are considered: Warm Deep Water (WDW), Weddell Sea Deep Water (WSDW), and Weddell Sea Bottom Water (WSBW). This approach allows investigation of the spatial distribution and temporal variability of the AABW varieties (WSDW and WSBW) close to their main formation area. The reader is referred to inspect Kerr et al. (2009a) for additional information regarding the procedures to determine the SWT indices and parameter weights defined (Table 2).

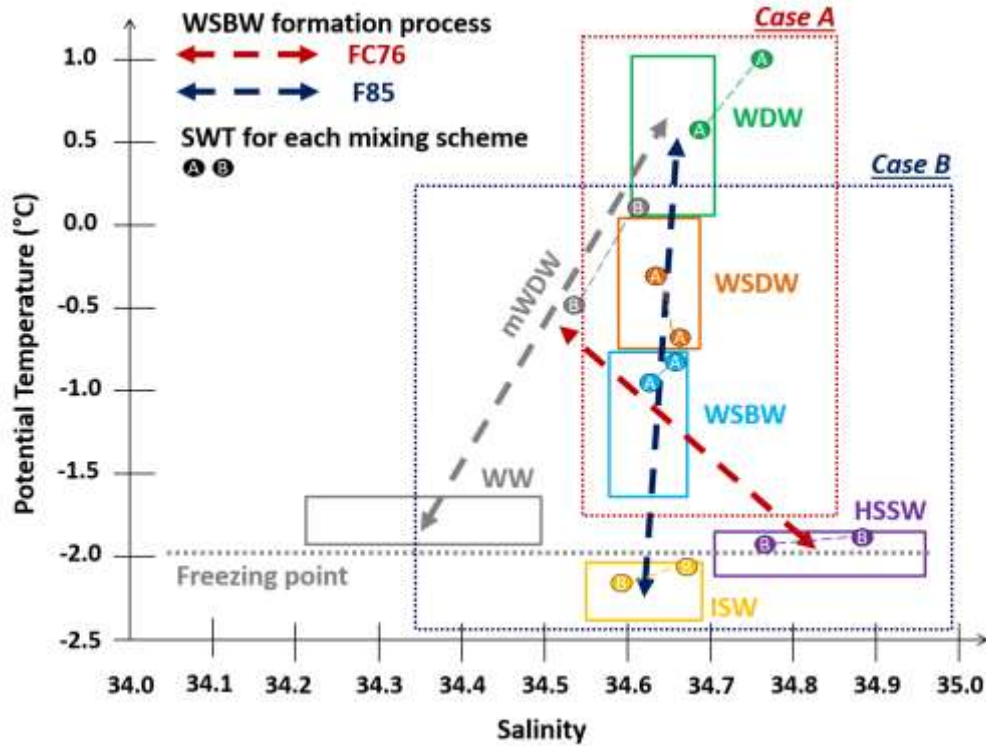


Figure 2. Mixing scheme for Weddell Sea Bottom Water (WSBW; light blue rectangle) formation in a potential temperature-salinity diagram. The horizontal dotted gray line is the surface freezing temperature. The gray and red dashed lines represent the mixing of Warm Deep Water (WDW; green rectangle) with Winter Water (WW; gray rectangle) to form modified-WDW (mWDW) and further mixing with High Salinity Shelf Water (HSSW; purple rectangle), representing the Foster and Carmack (1976) process (named as FC76). The dark blue dashed line represents WSBW formation by mixing of WDW/mWDW with Ice Shelf Water (ISW; yellow rectangle), representing the Foldvik et al. (1985) process (named as F85). *Case A* (red dotted rectangle) quantifies the mixture of WDW, Weddell Sea Deep Water (WSDW; orange rectangle) and WSBW in the Weddell Sea, whereas *Case B* (dark blue dotted rectangle) informs about the source water mass (i.e. mWDW, HSSW and ISW) contribution to form WSBW. The colored dots refer to the source water types (SWT) representing the water masses used for each approach (see Table 2). (For the interpretation of the references to color in this figure legend, the reader is referred to the web version of this article.)

Table 2. Range of source water types (SWT) and the parameter weights used in the OMP analyses performed, for each mixing scheme, through a Monte Carlo approach in the Weddell Sea. The parameter weights, for *Case A*, follow those determined by Kerr et al. (2009), whereas for *Case B* they were determined using Eq. 2 and a WOD13 data selection near the western and southern continental margins in the Weddell Sea. The dataset extracted to determine the weights for *Case B* was restricted to depths from 100 m to 600 m.

SWT	Case A				Case B			
Parameters	WDW	WSDW	WSBW	Weights	mWDW	HSSW	ISW	Weights
θ [°C]	0.5 1.0	-0.60 -0.30	-0.90 -0.80	11.5	-0.50 0.00	-1.95 -1.91	-2.20 -2.10	18.6
S	34.70 34.75	34.65 34.66	34.64 34.65	11.5	34.54 34.65	34.77 34.87	34.60 34.68	18.6
DO [$\mu\text{mol L}^{-1}$]	208 212	234 248	255 263	11.9 [#]	202.9 251.9	318.4 321.1	321.1 328.6	19.0 [#]

[#]Weight applied to the mass conservation.

The second mixing scheme considered (hereafter referred to as *Case B*) was performed for depths greater than 3000 m, which embrace the WSBW core (see for instance Fig. 3). In this approach, the SWT precursors of WSBW contributing to the mixture were: modified-Warm Deep Water (mWDW), High Salinity Shelf Water (HSSW), and Ice Shelf Water (ISW). Thus, the mixing scheme considered in *Case B* allows (a) to investigate the contribution changes of the WSBW source water masses and (b) to define which source water mass has the main influence in modulating the changes of the WSBW contribution throughout the period analyzed (see for instance Fig. 4c). We prefer to use a mWDW index instead of separate indices for WW and WDW because of (i) the limitation regarding the number of parameters to solve an additional mixing equation and (ii) the lack of other potential semi-conservative parameters to be used as water mass tracers in some of the cruises. However, additional OMP runs considering SWT indices for WW, WDW and one of the shelf water variety indicate negligible contribution of WW ($< 5\%$) to the total mixture (not shown). Considering the *Case B* applied here, the SWT indices (Tab. 2) were defined using the WOD13 data available nearby the western and southern continental shelf and shelf-break of the Weddell Sea. This follows a previous investigation of the water mass properties executed by Huhn et al. (2008) to better define the SWT indices for HSSW and ISW. Finally, only one SWT was used to represent each of the water masses considered, independently of the mixing schemes (Fig. 2; Tab. 2).

2.4. OMP sensitivity analysis

The OMP analysis does not consider temporal changes in the SWT definition. However, the method is widely suitable for identifying the temporal variability of water masses (e.g. Leffanue and Tomczak 2004; Tomczak and Liefvink 2005; Kerr et al.

2009a; Dotto et al. 2016). Thus, to avoid changes in SWT contributions that are related to an artifact of the method instead of real variations in the SWT fractions, a sensitivity analysis was performed to evaluate the robustness of the static SWT results. We opted for applying a Monte Carlo approach to randomly vary the SWT indices between the properties end-members (Table 2). A total of 100 OMP runs were performed with slightly modified SWT parameters considering the property range depicted in Table 2. Only the results that had a mass conservation residual below 10% were considered (Kerr et al., 2009a). In most cases, differences in the water mass contributions between the numerous OMP runs did not exceed 5%. Finally, the results presented in the following are the averaged contributions of all the 100 OMP runs performed. The minimum and maximum water mass contributions vary between 30-100%, with contribution values above 50% and 60% used hereafter as criterion to define a water mass layer and core, respectively.

3. Results

3.1. Weddell Sea deep water mass structure

The Weddell Sea deep water structure revealed by both hydrographic sections (WOCE SR4 and A12; Fig. 3) follows that expected for the region (e.g. Kerr et al. 2009a). The vertical water mass distribution shows: WDW contributing to the mixture in the upper 1500 m (Fig. 3a, d), WSDW occupies the layer between WDW and WSBW with a contribution higher than 60% around 2000 m (Fig. 3b, e), and WSBW cascades down the western continental slope (Fig. 3c) filling the near-bottom layer below 3500 m with a contribution higher than 60% (Fig. 3c, f). On average, the contributions to the total mixture between 1989–2011 (1984–2014) in the core of the WDW, WSDW and WSBW at WOCE SR4 (WOCE A12) were $79\pm11\%$ ($84\pm13\%$), $68\pm5\%$ ($68\pm5\%$),

$81 \pm 11\%$ ($75 \pm 9\%$), respectively (Fig. 4). The Weddell deep water mass contribution along the sections observed during each repeat cruise is shown in the Supplementary Material (Figs. S1 to S3).

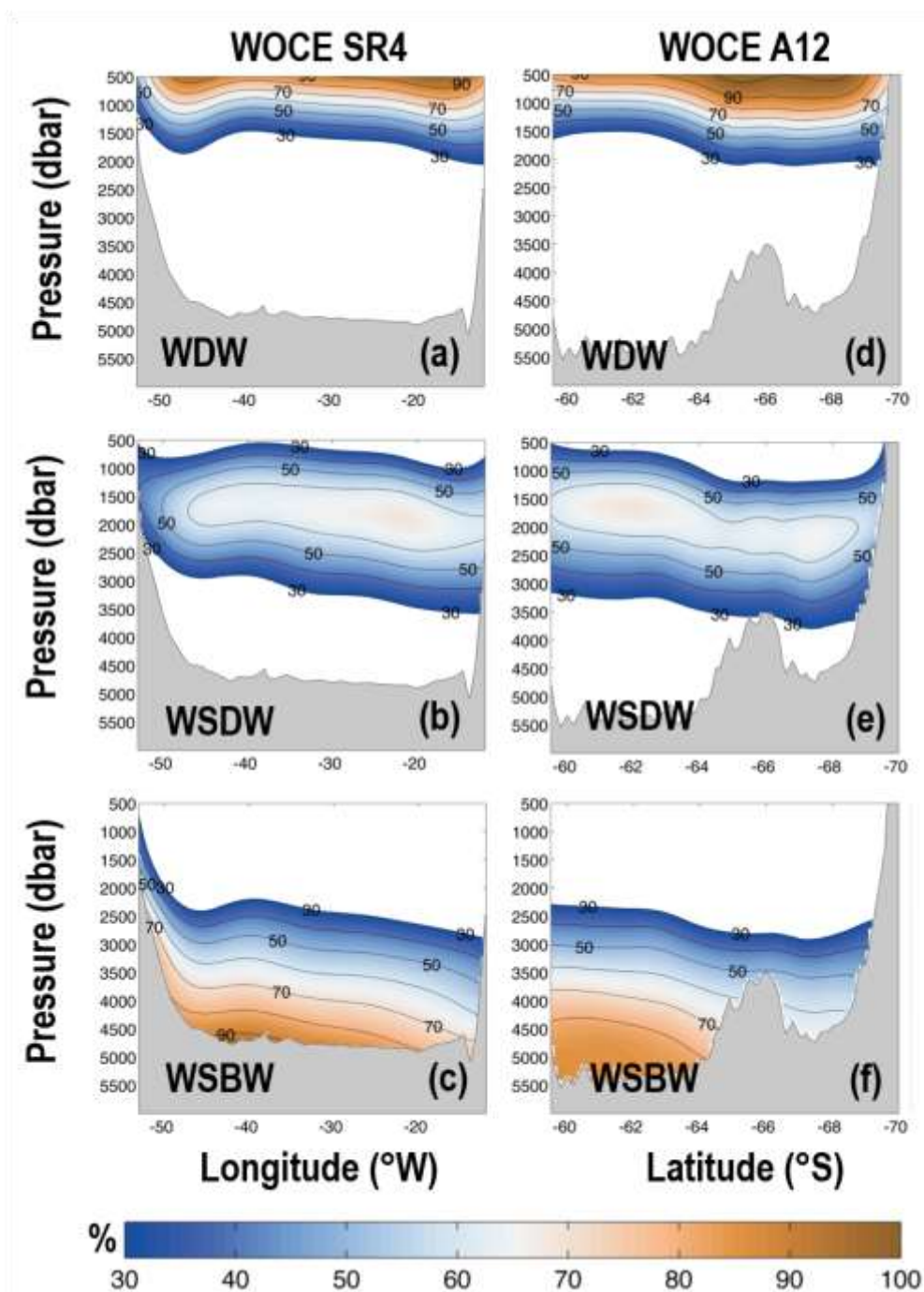


Figure 3. Averaged contribution to the Weddell Sea deep water masses (%) at the WOCE SR4 (left, 1989–2010) and WOCE A12 (right; 1984–2014) sections, respectively. (a, d) Warm Deep Water (WDW), (b, e) Weddell Sea Deep Water (WSDW), and (c, f) Weddell Sea Bottom Water (WSBW). (For the interpretation of the references to color in this figure legend, the reader is referred to the web version of this article.)

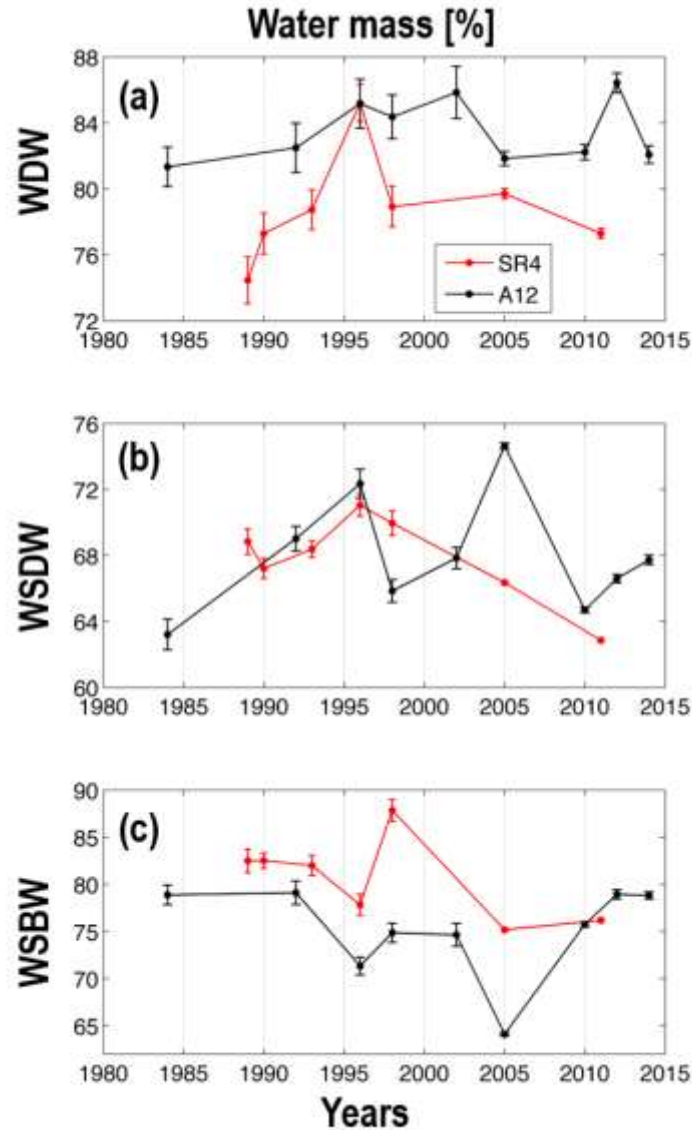


Figure 4. Time series (1984–2014) of the averaged contribution to the total mixture (%; *Case A*) in the core of the water mass (contribution > 60%) of (a) Warm Deep Water (WDW), (b) Weddell Sea Deep Water (WSDW), and (c) Weddell Sea Bottom Water (WSBW) on the vertical sections across the Weddell Gyre at the Greenwich Meridian (WOCE A12; black line) and in the Weddell Sea from Kapp Norvegia to Joinville Island (WOCE SR4; red line). The vertical bars indicate the water mass standard error. (For the interpretation of the references to color in this figure legend, the reader is referred to the web version of this article.)

3.2. Weddell Sea deep water mass variability

3.2.1. Water mass contribution to the total mixture

Temporal changes in the core (contribution > 60%) of the Weddell Sea deep water masses show a remarkable degree of interannual variability (Fig. 4). The WDW contribution in the Weddell Sea slightly increased (5-10%) for both repeat sections

during the whole period (Fig. 4a). A decreasing WSDW contribution is observed after 1996 at WOCE SR4, while at WOCE A12 the contribution variability was about ~10% (Fig. 4b). The increased WSDW contribution after 2010 at WOCE A12 is an interesting feature in the region. Furthermore, WSBW shows a pronounced decrease of ~8-15% between 1989–1996 and 1984–2005 in the central Weddell Sea and Greenwich Meridian repeat sections (Fig. 4c), respectively. In fact, the WSBW contribution continues to decrease until 2011 at WOCE SR4, considering that the high contribution observed in 1998 reflects the western half-section occupation in that particular year. Thereafter, a recovering period is observed at WOCE A12 for the WSBW contribution, characterized by an increment of about 15% in the last decade (Fig. 4c).

3.2.2. Water mass properties variability

To understand the observed variability of the Weddell Sea deep water mass contributions (section 3.2.1), the time series of the average hydrographic properties of each water mass were further analyzed using two approaches: (i) a layer based on neutral density (γ^n ; Jackett & McDougall, 1997) isopycnals (Fig. 5) and (ii) a layer based on the water mass core (i.e., contribution > 60%; Fig. 6). The first one allows further comparison with previous studies in the region that used similar methodology to distinguish the water mass layers (e.g. Fahrbach et al., 2011), whereas the second one allows the investigation of property changes in the layer of a more homogeneous water mass (or in its most pure form with less mixture interference from other water masses).

Time series of the averaged WDW properties ($28.1 \geq \gamma^n > 28.27 \text{ kg m}^{-3}$; Fig. 5 – left panels) show a warming of ~0.15°C until 1996 and a cooling of ~0.1°C afterwards, for both sections (Fig. 5a). Except for the anomalous year of 2005 that showed a drop (rise) of ~0.04 in the section A12 (SR4), changes in salinity are not pronounced

throughout the period analyzed (Fig. 5b). The WDW temperature fluctuations likely caused slight changes of the average density, with the decreasing temperature after 1996 linked with the densification of the WDW between 1996 and 2014 (Fig. 5c). The DO variability in the WDW indicates a reduction of $\sim 16 \mu\text{mol L}^{-1}$ until 1996 and a recovery afterwards with similar magnitude (Fig. 5d). The year 2012 shows the minimum DO value recorded in the time series at the WOCE A12 section (Fig. 5d).

When analyzing the average WDW properties only at the water mass core (Fig. 6 – left panels), the time series indicates slight changes in temperature ($\sim 0.1^\circ\text{C}$; Fig. 6a) and no significant fluctuations in salinity (~ 0.004 ; Fig. 6b), thus leading to small variability in terms of density (Fig. 6c). On the other hand, DO decreased by $\sim 8 \mu\text{mol L}^{-1}$ in WOCE A12 until 2005 (except for the year 1998), while in WOCE SR4 the decrease in DO of the same magnitude stopped in 1996 (Fig. 6d). Afterwards, one observes a DO increase of $\sim 5 \mu\text{mol L}^{-1}$ in the WDW at the WOCE SR4 section. The same magnitude of the DO increase can be observed at WOCE A12, even with the abrupt drop in DO during the year 2011 (Fig. 6d).

Time series of the average WSDW properties ($28.27 \geq \gamma^n > 28.40 \text{ kg m}^{-3}$; Fig. 5 – center panels) also indicate an interannual variability. Although minor changes were observed in the average temperature and salinity during the time, it is possible to infer an increase in temperature and salinity starting after the mid-1980s (Fig. 5e-f). The year 1998 was marked by the lowest temperature and highest salinity in the central Weddell Sea (however, care should be taken in the interpretation of the patterns of variability as the WOCE SR4 section was not completely occupied during this year). The oscillations in the average temperature and salinity are reflected in the variability of WSDW average density, with an opposing phase between the sections analyzed (Fig. 5g). In the

WOCE A12, less dense WSDW was observed during the 1980s and after the year 2000, and a denser variety of WSDW appeared between 1995 and 2000 (Fig. 5g). The opposing pattern, with less variability, was observed in WOCE SR4. On the other hand, changes in the DO time series occur in phase for both sections and are marked by higher variability (Fig. 5h), with a similar pattern to that reported for WDW (Fig. 5d).

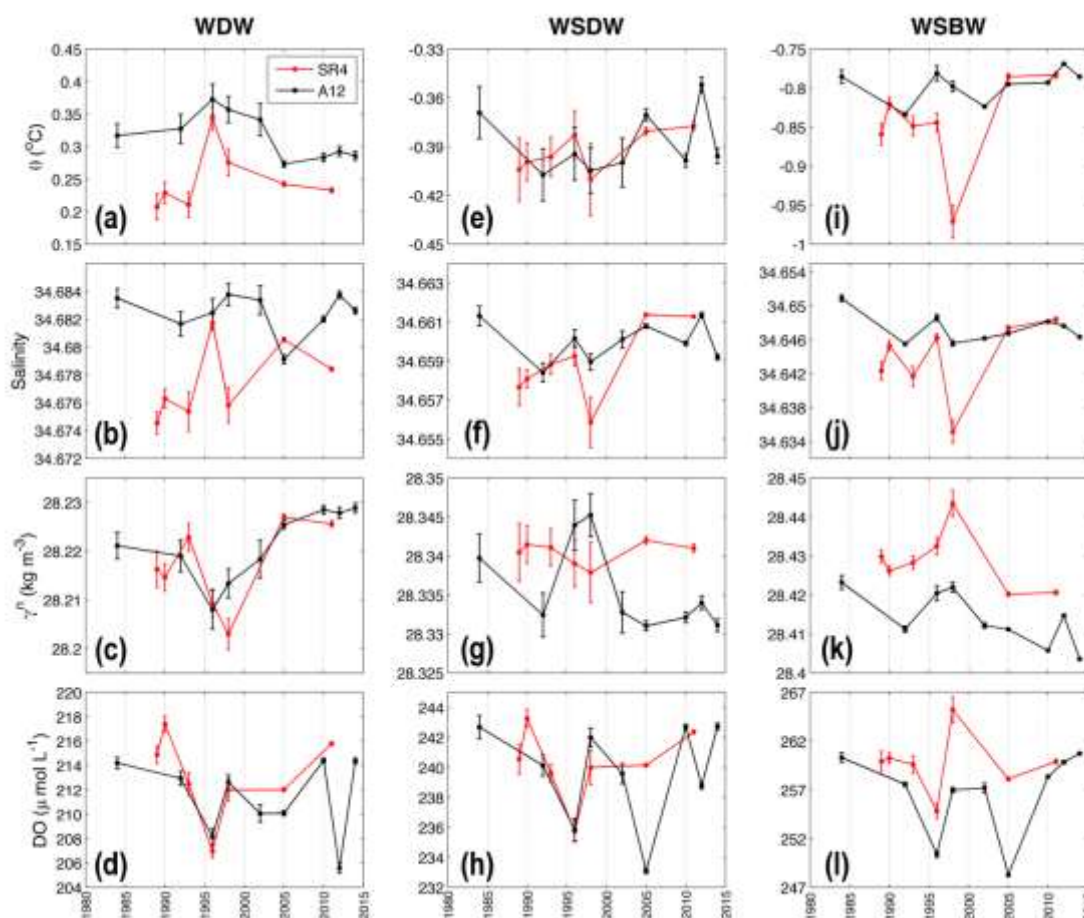


Figure 5. Time series (1984–2014) of the average (**top**) potential temperature ($^{\circ}\text{C}$), (**2nd row**) salinity, (**3rd row**) neutral density (γ^n ; kg m^{-3}), and (**bottom**) dissolved oxygen (DO; $\mu\text{mol L}^{-1}$) of (**left**) Warm Deep Water (WDW; $28.1 \geq \gamma^n > 28.27 \text{ kg m}^{-3}$), (**center**) Weddell Sea Deep Water (WSDW; $28.27 \geq \gamma^n > 28.40 \text{ kg m}^{-3}$) and (**right**) Weddell Sea Bottom Water (WSBW; $\gamma^n \geq 28.40 \text{ kg m}^{-3}$) on the sections across the Weddell Gyre at the Greenwich Meridian (WOCE A12; black line) and across the Weddell Sea from Kapp Norvegia to Joinville Island (WOCE SR4; red line). The neutral density criterion informed was used to determine the average of each hydrographic property of each of the Weddell Sea deep water layers. The vertical bars indicate the properties standard error. (For the interpretation of the references to color in this figure legend, the reader is referred to the web version of this article.)

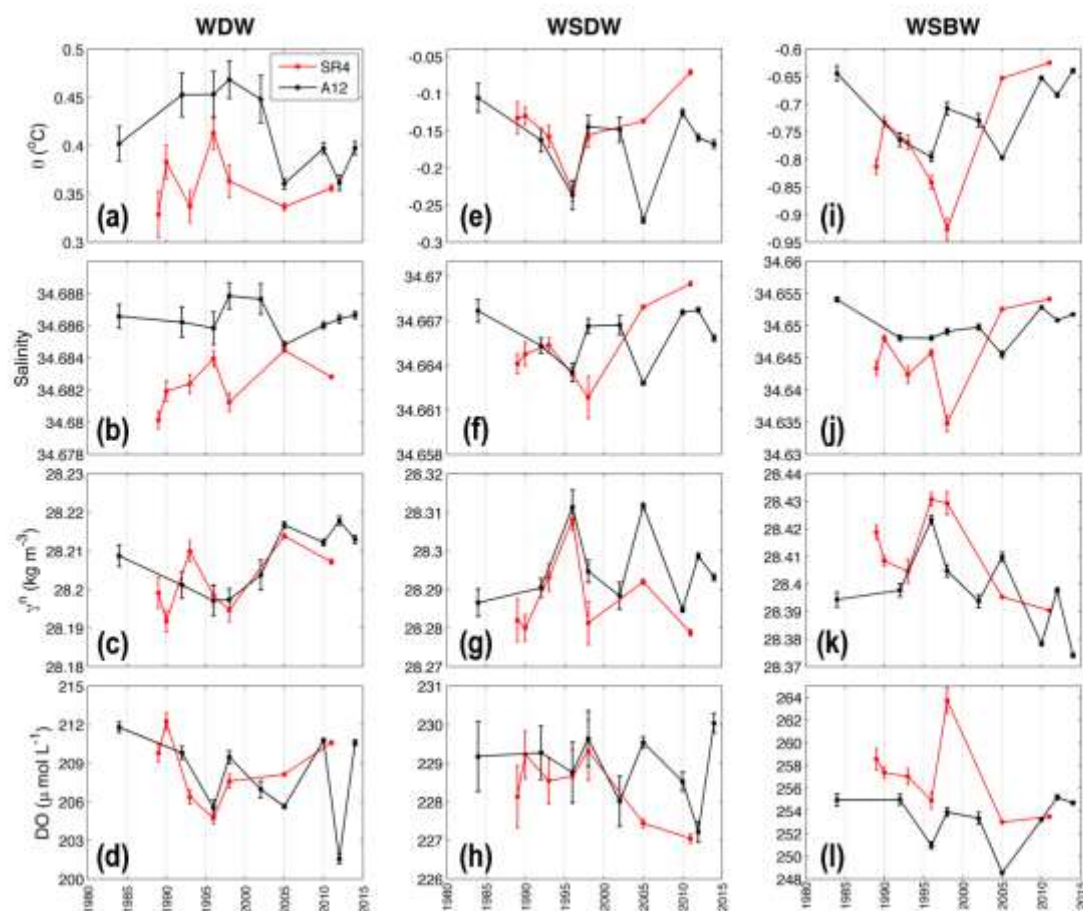


Figure 6. Time series (1984–2014) of the average (**top**) potential temperature ($^{\circ}\text{C}$), (**2nd row**) salinity, (**3rd row**) neutral density (γ^n ; kg m^{-3}), and (**bottom**) dissolved oxygen (DO; $\mu\text{mol L}^{-1}$) in the core (water mass contribution $> 60\%$; see Fig. S1–S3) of (**left**) Warm Deep Water (WDW), (**center**) Weddell Sea Deep Water (WSDW) and (**right**) Weddell Sea Bottom Water (WSBW) on the sections across the Weddell Gyre at the Greenwich Meridian (WOCE A12; black line) and across the Weddell Sea from Kapp Norvegia to Joinville Island (WOCE SR4; red line). The vertical bars indicate the properties standard error. (For the interpretation of the references to color in this figure legend, the reader is referred to the web version of this article.)

In contrast to the average WSDW properties based on neutral density layers, changes in the WSDW core are more pronounced (Fig. 6 – center panels). The WSDW average temperature decreased by $\sim 0.10\text{--}0.15^{\circ}\text{C}$ until 1996 and increased by $\sim 0.18^{\circ}\text{C}$ afterwards (Fig. 6e; obvious in WOCE SR4 and less evident in WOCE A12 because of the lowest averaged temperature recorded in 2005), while salinity slightly increased by ~ 0.005 during the whole period in section SR4 (Fig. 6f). Thus, our results unveil two quite distinct periods (Fig. 6g): 1984–1996 (increasing density) and 1996–2014 (decreasing density). DO decreases by $\sim 2 \mu\text{mol L}^{-1}$ in WOCE SR4 after the 1990s,

while a high degree of DO variability is observed in WOCE A12 with values close to those observed in the early 1990s for year 2014 (Fig. 6h).

The variability observed in the WSBW properties ($\gamma^n \geq 28.40 \text{ kg m}^{-3}$; Fig. 5 – right panels) is small for average temperature, except for the coldest temperatures recorded in the year 1998 on WOCE SR4 that reflects the partial occupation of the section (Fig. 5i). Average salinity decreased by ~ 0.004 at the Greenwich Meridian, whereas changes on WOCE SR4 reveal small oscillations (Fig. 5j). Despite the year 1998, both temperature ($\sim 0.05^\circ\text{C}$) and salinity (~ 0.06) increased in the inner Weddell Sea (Fig. 5i-j). The WSBW average density decreased on WOCE A12 when considering the whole period, whereas the density increased in the center Weddell Gyre between the start of the time series until 1998 (this increase is also noticeable in the WOCE A12) and decreased afterwards (Fig. 5k). The average DO in WSBW shows a high level of interannual variability (Fig. 5l). The year 1998 is marked by the highest average DO in WOCE SR4 (again reflecting the half-section occupation), whereas a pronounced increase in the DO concentration after 2005 is observed in WOCE A12 (Fig. 5l). Thus, one can infer that after 2005 (inclusive) the WSBW formation recovered, using DO as a proxy to refer to recent water mass ventilation, i.e., indicating years of strong renewal of the WSBW layer (Fig. 5l).

The variability observed only in the WSBW core (Fig. 6 – right panels) shows that both average temperature ($\sim 0.15^\circ\text{C}$) and salinity (~ 0.005) decreased until 1996 on WOCE SR4, followed by an increase of $\sim 0.2^\circ\text{C}$ and ~ 0.01 , respectively (Fig. 6i-j). In spite of the high variability observed, the WSBW density time series reveals a lightening of that water mass starting in the mid-1990s (Fig. 6k), in parallel with a reduction of DO concentration of $\sim 5\text{--}8 \mu\text{mol L}^{-1}$ during ~ 20 years (1984–2005) in both sections (Fig. 6l). A rapid renewal of the WSBW layer, occurring within ~ 10 years,

after that period is indicated by increased values of DO with the same magnitude previously reported for the beginning of sampling on section WOCE A12 (Fig. 6l).

3.3. Weddell Sea Bottom Water sources and changes

The WSBW core (contribution $> 60\%$), considering depths greater than 3000 m, was composed on average of $70\pm 5\%$ and $71\pm 3\%$ of mWDW, $19\pm 3\%$ and $20\pm 1\%$ of HSSW, and $11\pm 7\%$ and $9\pm 4\%$ of ISW (Fig. 7) on WOCE SR4 and WOCE A12, respectively (Fig. 4). As the mWDW and Dense Shelf Waters (sources of the WSBW) contributions changed throughout the time, it is possible to evaluate which physical processes potentially influenced the changes of WSBW (Fig. 8).

The mWDW contribution increased by $\sim 6\text{--}8\%$ through the period analyzed (Fig. 8a), same as reported for WDW quantified in *Case A* (Fig. 4a). Also, the mWDW contribution decreased by $\sim 4\%$ after 2005 on WOCE A12. The mWDW contribute to WSBW the most in year 2005 for both sections (Fig. 8a). As the OMP analysis is constrained by mass conservation in the mixing scheme, the changes observed, when combining the Dense Shelf Waters contributions (Fig. 8b), are mirrored to mWDW contribution (Fig. 8a).

Although the contribution of both shelf-sources reflects intense interannual variability, a clear decrease of $\sim 5\%$ of Dense Shelf Waters is observed between 1984–2005, followed by an increase of $\sim 3\%$ in the section WOCE A12 (Fig. 8b). Separating the WSBW shelf-sources in HSSW and ISW, one observes an increasing HSSW contribution of $\sim 3\%$ in the inner Weddell Sea (except for the drop observed in 1998) and no significant variations at the Prime Meridian (Fig. 8c). On the other hand, the contribution of ISW decreases between 6–8% for both sections (again excluding the year 1998 for WOCE SR4) until 2005 (Fig. 8d). After that, the ISW contribution to the

WSBW mixture increases by ~2%, which is noticeable on the WOCE A12 section (Fig. 8d).

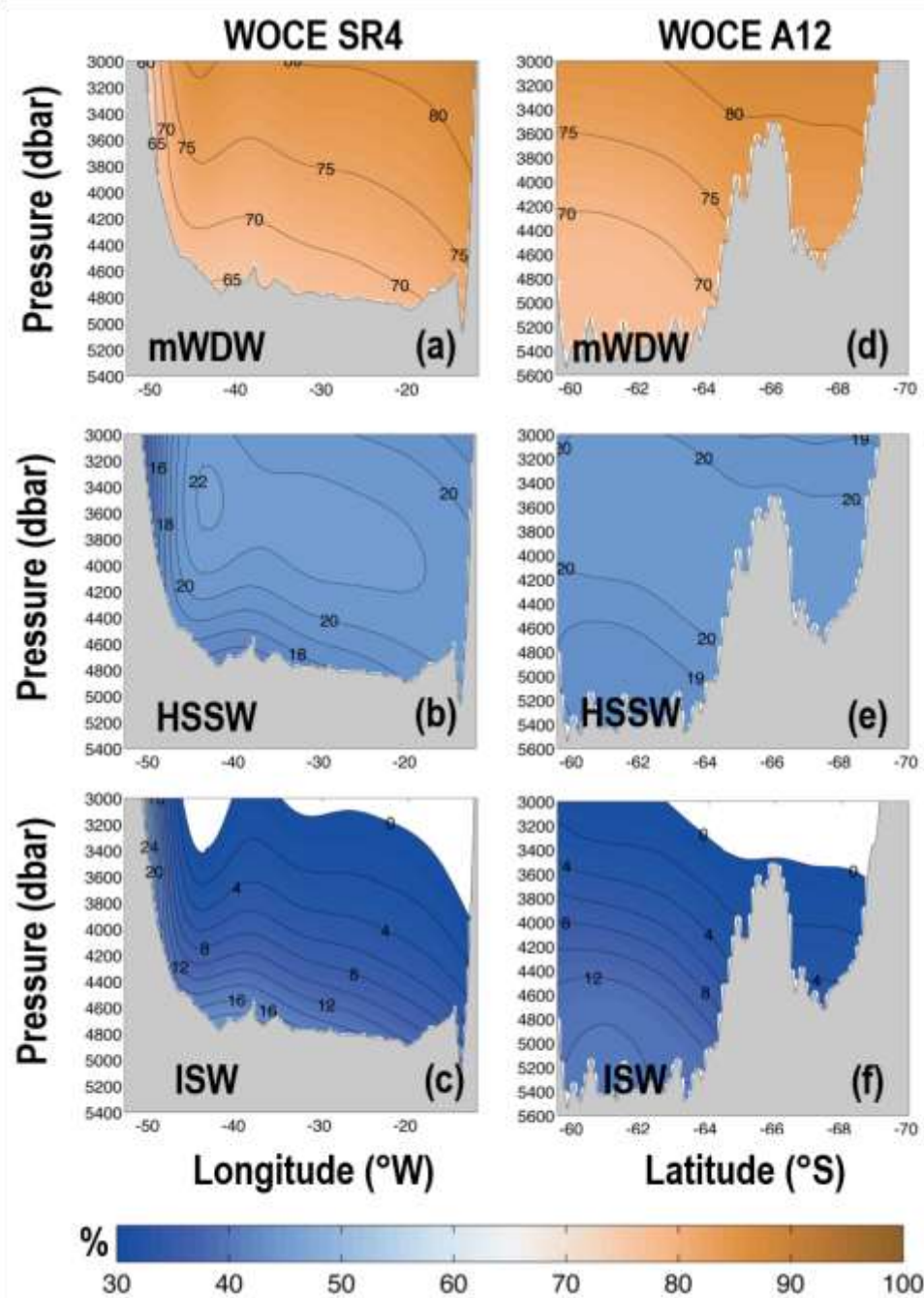


Figure 7. Average contribution (%) of the source water masses of Weddell Sea Bottom Water to the layer with contributions > 50% (see Fig. 3c and f) on the sections WOCE SR4 (left panels, 1989–2010) and WOCE A12 (right panels; 1984–2014), respectively, (a, d) Warm Deep Water (WDW), (b, e) High Salinity Shelf Water (HSSW), and (e, f) Ice Shelf Water (ISW). (For the interpretation of the references to color in this figure legend, the reader is referred to the web version of this article.)

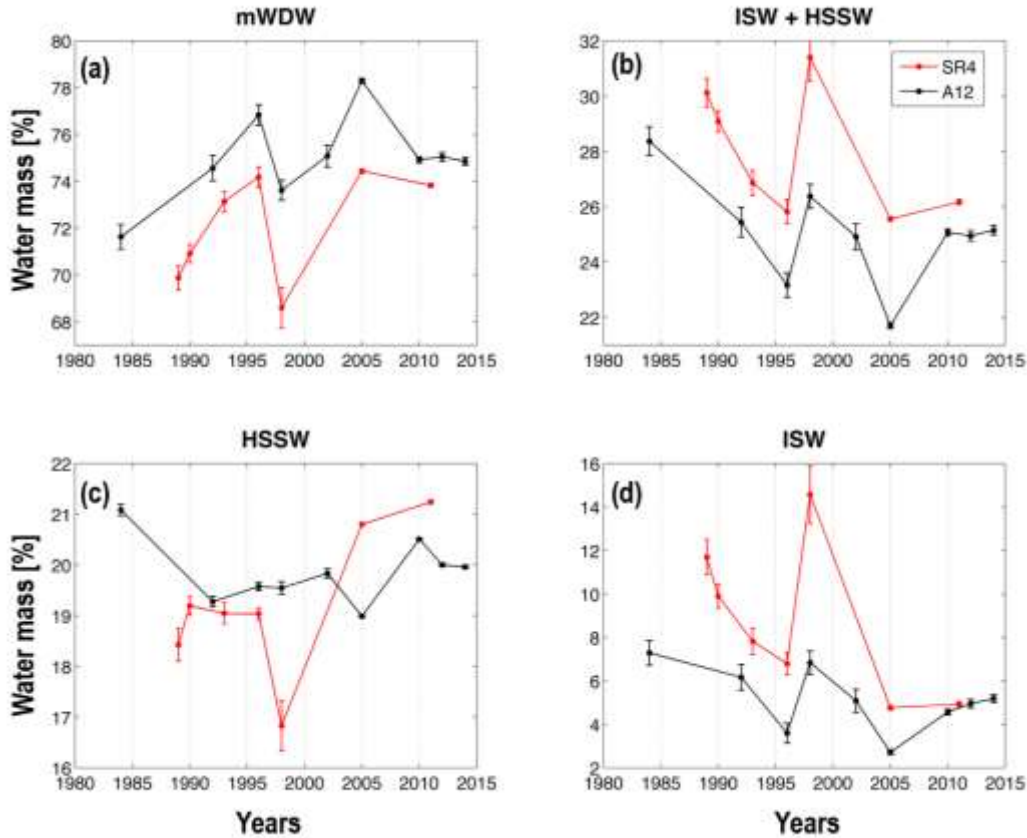


Figure 8. Time series (1984–2014) of the average source water mass contribution - (a) modified-Warm Deep Water (mWDW), (b) Dense Shelf Waters (merged contribution of HSSW and ISW), (c) High Salinity Shelf Water (HSSW), and (d) Ice Shelf Water (ISW) to the total mixture (%; *Case B*) in the Weddell Sea Bottom Water (Fig. 3c and f) on the section across the Weddell Gyre at the Greenwich Meridian (WOCE A12; black line) and across the Weddell Sea from Kapp Norvegia to Joinville Island (WOCE SR4; red line). The vertical bars indicate the water mass standard error. (For the interpretation of the references to color in this figure legend, the reader is referred to the web version of this article.)

4. Discussion and Conclusion

The Weddell Sea deep water mass structure presented in Figure 3 agrees with that previously described by Kerr et al. (2009a) as expected, because both studies used the same methodology and datasets overlap during part of the time series. However, the use of a more appropriate sensitive analysis here, through a Monte Carlo approach varying the SWT, causes changes in the average contribution and the depth-limits of WSDW boundary with other water masses when compared to the previous study. Thus, the WDW/WSDW and WSDW/WSBW boundaries changed approximately by 500 m from those previously reported by Farhbach et al. (2004; 2011). The authors split the

water mass layers in the Weddell Sea using the isopycnal (isotherm) boundary of 28.27 kg m^{-3} (0°C) and 28.40 kg m^{-3} (-0.7°C), which changes the depth of the water mass mixing zone between the studies. However, the combined use of temperature, salinity, and DO, to distinguish the layer of the purest form of the water masses (i.e., its high percentage of mixture), reveals further important aspects regarding how a particular water mass evolves through time. That was sometimes masked using the above parameter thresholds. The temporal variability observed in the contribution to Weddell Sea deep waters (Sect. 3.2.1) is likely caused by a combination of changes in (i) the source water mass properties (Meredith et al., 2011; Azaneu et al., 2013; Schmidt et al., 2014), (ii) the Weddell Gyre circulation and dynamics (Meredith et al., 2008; Jullion et al., 2014), and (iii) the production and export of Dense Shelf Waters from the shelf (Kerr et al. 2012a; Heywood et al., 2014). In fact, shifts in WSBW hydrographic properties towards less dense varieties (Figs. 5k) likely equate to less WSBW being produced over time, which is further supported by the decreasing of DO concentration (i.e., less ventilation) in the bottom layer (Fig. 6k) of the Weddell Sea.

The increasing contribution of WDW (Fig. 4a) during the three decades analyzed is possibly reflecting the intensification of the Southern Ocean winds driven by the positive long-term trend of the Southern Annular Mode (Jullion et al., 2010). That mechanism may play a role on the southward displacement of the fronts of the Antarctic Circumpolar Current (Sokolov and Rintoul, 2009) and on the intensity of mesoscale eddies in the Southern Ocean (Meredith, 2016). Both processes can possibly influence the inflow of Circumpolar Deep Water (CDW—a water mass precursor of WDW) into the Weddell Sea. Thus, the processes may allow the WDW contribution to increase in phase and at similar rates both along the Prime Meridian and in the inner Weddell Sea (Fig. 4a; Table 3). It is also important to highlight that the temporal

changes in the WDW layer are affected by a mixture of different CDW-inflows from the Antarctic Circumpolar Current and recirculated-WDW in the Prime Meridian region (Ryan et al., 2016). Hence, the WDW core gradually merges and becomes more homogeneous towards the west (Leach et al., 2011), such as observed by the property time series (Fig. 6 – left panels). In addition, the WDW increased availability within the Weddell Gyre during the three decades analyzed (Fig. 4a) has changed the WSBW layer, which now unveils a higher percentage of the former as part of its composition (Fig. 8a). In fact, that observation agrees with the reported declining ventilation of the Antarctic deep and bottom waters (Huhn et al., 2008), which was simultaneously manifested in the Weddell Sea by a decrease of ~20% in the WSBW contribution (Kerr et al. 2009a), the AABW volume contraction (Azaneu et al., 2013), and a decreasing trend in DO for the bottom layer (van Heuven et al., 2014).

The temporal changes of the WSDW contribution (Fig. 4b) reveal a marked interannual variability (sometimes varying the contribution up to ~10%), which is likely driven by small changes in the rate its precursor water masses mix during the formation process (Daae et al., 2009), but also due to changes in the internal diapycnal mixing (Heywood et al., 2002; Sloyan, 2005) and Southern Ocean circulation (Naveira Garabato et al., 2014). This behavior is more obvious on the WOCE A12 section as that region is more dynamically active because of both the steep bathymetry and the vicinity to the inflow of CDW into the Weddell Sea (~20-30°E; e.g. Gouretski and Danilov, 1993; Schröder and Fahrbach, 1999; Ryan et al., 2016). Furthermore, the rapid renewal of the WSBW layer observed after 2005 at the Prime Meridian (Fig. 4c) is also seen in the WSDW layer after 2010 (Fig. 4b). The ~5 years lag can be an indicator for the mixing time scale between WSDW and WSBW, although further investigation is

needed due to the relatively sparse temporal resolution combined with the strong temporal variability of the properties of those water masses.

The decreasing WSDW contribution in WOCE SR4 is within the same range of the temporal variability as reported for the Prime Meridian (Fig. 4b). This suggests that the Weddell Gyre circulation can damp temporal changes within the Weddell Sea, but it also demonstrates that WSDW (the most voluminous water mass filling the Weddell Basin) is not completely matured. In fact, Robertson et al. (2002) pointed out that, although the average WSDW potential temperature between 1500 m and 3500 m was higher in the 1990s than in the 1970s, high variability in the data prevented the identification of a well-defined temporal trend. Moreover, changes in salinity were not observed in the deep layer of the Weddell Sea ($\gamma^n > 28.27 \text{ kg m}^{-3}$) fusing a dataset of ~50 years (1958–2010; Azaneu et al., 2013), which is an intriguing observation given the recent freshening of AABW varieties and AABW shelf-sources reported for sites all around the Antarctic continent (Aoki et al., 2005; Rintoul, 2007; Hellmer et al., 2011; Jullion et al., 2013; Dotto et al., 2016). Hence, a swifter circulation in the Weddell Sea (Meredith et al., 2011) can also contribute to an enhanced export of WSDW, newly formed in the northwestern Weddell Sea. That young water mass potentially carries out of the Weddell Sea the freshening signal resulting from changes in Dense Shelf Waters properties (Azaneu et al., 2013) due to ocean-ice interactions (Cook et al., 2005; Pritchard and Vaughan, 2007; Chen et al., 2008; Rignot et al., 2008; Cook et al., 2016). Thus, preventing those time changes in the properties of the WSDW sources leads to a more consistent impact on their contribution to the total mixture in the inner Weddell Sea. Moreover, the time series currently available are not long enough yet to allow for a distinction of the signals and further conclusions on the drivers of the WSDW temporal variability.

Changes in the WSBW contribution (Fig. 4c) agree with the ~20% decrease previously reported by Kerr et al. (2009a) until the end of the 1990s, but the WSBW formation strength recovers afterwards. The pattern reversal is clearly visible by the increased WSBW contribution after 2005 in WOCE A12, but not apparently manifested in the inner Weddell Sea. However, the vigorous increase of WSBW at the Prime Meridian indicates that other dense bottom water sources are influencing the region (e.g. Couldrey et al, 2013). In this context, the changes observed in the WSBW precursors (Fig. 8) indicate that Dense Shelf Waters are responsible for modulating the WSBW variability. This is particularly true because the mWDW contribution to the WSBW layer (Fig. 8a) and the strength of the WDW core in the Weddell Sea (Fig. 4a) both have increased throughout the time series. The Dense Shelf Waters (Fig. 8b) contribution unveils a behavior with similar temporal changes as in the WSBW contribution (Fig. 4c) and changes in the DO content of the WSBW layer (Fig. 6l). It is interesting to note that even the Dense Shelf Waters modulate the WSBW temporal changes when separating the contribution into HSSW and ISW. The variability of the WSBW in WOCE SR4 (Fig. 4c) is mostly driven by the increasing (decreasing) contribution of HSSW (ISW) (Fig. 8c), whereas ISW modulates the WSBW changes in WOCE A12 after 2005 since HSSW monotonically changes through time (Fig. 8d).

The newly-formed WSBW, present in the region of WOCE A12, likely results from an increasing contribution of other AABW varieties formed in the Indian Sector of the Southern Ocean, being advected towards the Prime Meridian as previously proposed by Meredith et al. (1999; 2000) and Jullion et al. (2014). The potential temperature-salinity diagram (Fig. 9), considering AABW varieties with $\gamma^n \geq 28.40 \text{ kg m}^{-3}$ at 30°E, 0°, and the inner Weddell Sea, shows that the AABW variety marked as WSBW on WOCE A12 is derived from the Indian Ocean-variety of AABW after 2005 (Fig. 9c and

d), which has a density different from the varieties formed within the Weddell Sea. However, no distinction of the AABW sources is evident during the 1990s, because AABW varieties at the Prime Meridian and in the Indian Sector followed roughly the same isopycnals (Fig. 9a and b). It is worth mentioning that both the different vertical resolution of each datasets (e.g., bottle and CTD) used and the possible inter-cruise systematic differences have a negligible effect on this conclusion (e.g., salinity differences are within the same range of the deviation of the label standard seawater salinity in laboratory measurements). Therefore, the observations indicate that prior to 2005 the bottom waters were well-mixed in the region and/or no pulses of AABW of Indian Ocean origin occurred during that period.

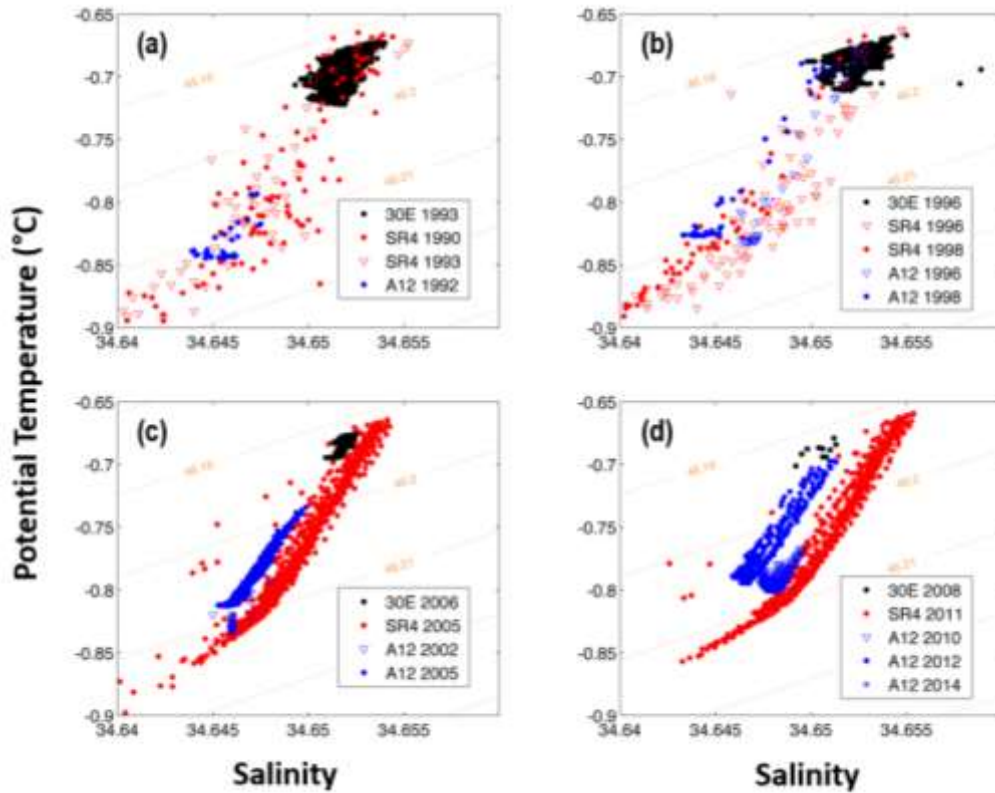


Figure 9. Potential temperature-salinity diagrams considering the near-bottom layer ($\gamma^n \geq 28.4 \text{ kg m}^{-3}$) and latitude greater than 60°S at the WOCE SR4 (inner Weddell Sea; red symbols), WOCE A12 (Prime Meridian; blue symbols), and WOCE I6S (30°E ; black dots) repeat sections. The dataset used for WOCE SR4 and WOCE A12 is the same used to perform the OMP analysis. The year of the measurement is indicated by the legend for each respective section, grouped in nearest sampling years: (a) 1990–1993, (b) 1996–1998, (c) 2002–2006, and (d) 2008–2014. The isopycnals refers to σ_4 . (For the interpretation of the references to color in this figure legend, the reader is referred to the web version of this article.)

In addition, the source water mass contributions to WSBW are redefined here to be composed by a mixture of $71\pm4\%$ of mWDW, $19\pm2\%$ of HSSW, and $10\pm6\%$ of ISW (Fig. 7) for the whole Weddell Sea, with almost no difference between both regions analyzed. These results update the proportion of the sources forming WSBW, previously estimated to be approximately 65% of WDW and 35% of Dense Shelf Waters (Gill, 1973; Carmack, 1974). Also, assuming that Dense Shelf Waters are the youngest water masses of the WSBW precursors, our results corroborate with earlier estimates that 12% to 30% of the bottom waters in the Weddell Sea are newly-formed (Carmack and Foster, 1975).

In summary, extending the time series analysis of Weddell Sea deep and bottom water properties to around three decades of investigation (even considering the sparse temporal resolution) allows us to better understand the WSBW origin in the Weddell Sea and how it has been evolved (transformed/modified) over time. This study shows that shifts in WSBW properties towards less dense varieties in the Weddell Sea likely equate to less WSBW being produced over time. The decline of WSBW volume observed until the 1990s ceased around 2005 and likely recovered thereafter (particularly in the WOCE A12 region, due to pulses of AABW from the Indian Ocean). The increase of the WSBW contribution results from changes in the proportion of WDW and Dense Shelf Waters, while the latter drive and modulate the recent WSBW variability. As a result, WSBW present in the Weddell Basin is now composed by 71% of WDW and 29% of Dense Shelf Waters.

Finally, the distinction between the AABW varieties within the entire Southern Ocean is still a complex issue to be solved due to the proximity of their property values. However, as particular ocean-ice processes with different time scales are responsible for modifying the regional varieties of AABW in diverse ways, further efforts should be

taken to correctly interpret the signals of recent AABW warming and freshening that spread towards the global ocean (Bindoff and Hobbs, 2013). In this context, the Southern Ocean environment (mostly during austral winter when AABW formation in particular occurs) imposes a barrier for comprehensive synoptic observations around the continent even in the light of modern technologies and techniques. Nevertheless, some progress has been achieved to observe the ocean under the ice as this task has been receiving special attention from the international community (Meredith et al., 2013; 2015). Unfortunately, ocean models and reanalysis products normally lack to properly represent the AABW layer as well as its properties and formation processes (Kerr et al. 2009b; Kerr et al., 2012a, b; Azaneu et al., 2014; Dotto et al., 2014). Nevertheless, a recent investigation on the representation of deep convection occurring in ocean reanalysis products revealed that the mechanism of AABW formation in the Indian Sector of the Southern Ocean is plausible by combining both continental shelf convection and the export of Dense Shelf Waters to the open ocean (Aguar et al., 2017). These findings indicate that observations and modeling should be used together to fill the gaps and better understand the processes controlling the formation and variability of AABW regional varieties.

5. Acknowledgements

This work is dedicated to the memory of Eberhard Fahrbach, without his vision and efforts, this most valuable data set of the Weddell Sea covering more than three decades would not exist. This study provides a contribution to the activities of the Brazilian High Latitudes Oceanography Group (GOAL), which is part of the Brazilian Antarctic Program (PROANTAR). GOAL has been funded by and/or has received logistical support from the Brazilian Ministry of the Environment (MMA), the Brazilian

Ministry of Science, Technology, Innovation and Communication (MCTIC), and the Council for Research and Scientific Development of Brazil (CNPq) through grants from the Brazilian National Institute of Science and Technology of Cryosphere (INCT-CRIOSFERA; CNPq grants n° 573720/2008-8 and 465680/2014-3), NAUTILUS (CNPq grant n° 405869/2013-4), and CAPES/CMAR2 (CAPES grant n° 23038.001421/2014-30) projects. R. Kerr and M. M. Mata acknowledge CNPq researcher grants n° 302604/2015-4 and 306896/2015-0, respectively. T. S. Dotto was funded by a CNPq PhD grant n° 232792/2014-3. We are grateful for the constructive comments provided by two anonymous reviewers which substantially improved the manuscript.

6. References

- Aguiar, W.C., Mata, M. M. & Kerr, R., (2017; accepted for OS). On the deep convection events and Antarctic Bottom Water formation in ocean reanalysis products. *Ocean Science Discussions*, doi:10.5194/os-2017-9.
- Aoki, S., Rintoul, S. R., Ushio, S., Watanabe, S., & Bindoff, N. L. (2005). Freshening of the Adélie Land Bottom water near 140 E. *Geophysical Research Letters*, 32(23).
- Azaneu, M., Kerr, R., Mata, M. M., & Garcia, C. A. (2013). Trends in the deep Southern Ocean (1958–2010): Implications for Antarctic Bottom Water properties and volume export. *Journal of Geophysical Research: Oceans*, 118(9), 4213-4227.
- Azaneu, M., Kerr, R., & Mata, M. M. (2014). Assessment of the representation of Antarctic Bottom Water properties in the ECCO2 reanalysis. *Ocean Science*, 10(6), 923.
- Bindoff, N. L., & Hobbs, W. R. (2013). Oceanography: Deep ocean freshening. *Nature Climate Change*, 3(10), 864-865.
- Carmack, E. C. (1974). A quantitative characterization of water masses in the Weddell Sea during summer. *Deep Sea Research and Oceanographic Abstracts*. Vol. 21, No. 6, pp. 431-443.
- Carmack, E. C., & Foster, T. D. (1975a). On the flow of water out of the Weddell Sea. *Deep Sea Research and Oceanographic Abstracts*. Vol. 22, No. 11, pp. 711-724.
- Carmack, E. C., & Foster, T. D. (1975b). Circulation and distribution of oceanographic properties near the Filchner Ice Shelf. *Deep Sea Research and Oceanographic Abstracts* Vol. 22, No. 2, pp. 77-90.
- Chen, J. L., Wilson, C. R., Tapley, B. D., Blankenship, D., & Young, D. (2008). Antarctic regional ice loss rates from GRACE. *Earth and Planetary Science Letters*, 266(1), 140-148.
- Comiso, J. C. and Gordon, A. L.: Recurring polynyas over the Cosmonaut Sea and the Maud Rise, *J. Geophys. Res.-Ocean.*, 92, 2819–2833, <https://doi.org/10.1029/JC092iC03p02819>, 1987.
- Cook, A. J., Fox, A. J., Vaughan, D. G., & Ferrigno, J. G. (2005). Retreating glacier fronts on the Antarctic Peninsula over the past half-century. *Science*, 308(5721), 541-544.
- Cook, A. J., Holland, P. R., Meredith, M. P., Murray, T., Luckman, A., & Vaughan, D. G. (2016). Ocean forcing of glacier retreat in the western Antarctic Peninsula. *Science*, 353(6296), 283-286.
- Couldrey, M. P., Jullion, L., Naveira Garabato, A. C., Rye, C., Herráiz-Borreguero, L., Brown, P. J., ... & Speer, K. L. (2013). Remotely induced warming of Antarctic Bottom Water in the eastern Weddell gyre. *Geophysical Research Letters*, 40(11), 2755-2760.

Daae, K. L., Fer, I., & Abrahamsen, E. P. (2009). Mixing on the continental slope of the southern Weddell Sea. *Journal of Geophysical Research: Oceans*, 114(C9).

De Lavergne, C., Palter, J. B., Galbraith, E. D., Bernardello, R., & Marinov, I. (2014). Cessation of deep convection in the open Southern Ocean under anthropogenic climate change. *Nature Climate Change*, 4(4), 278-282.

Dotto, T. S., Kerr, R., Mata, M. M., Azaneu, M., Wainer, I. E. K. C., Fahrbach, E., & Rohardt, G. (2014). Assessment of the structure and variability of Weddell Sea water masses in distinct ocean reanalysis products. *Ocean Science*, 10, 523–546, 2014, 10, 523-546.

Dotto, T. S., Kerr, R., Mata, M. M., & Garcia, C. A. (2016). Multidecadal freshening and lightening in the deep waters of the Bransfield Strait, Antarctica. *Journal of Geophysical Research: Oceans*, 121(6), 3741-3756.

Driemel, A., Fahrbach, E., Rohardt, G., Beszczynska-Möller, A., Boetius, A., Budéus, G., Cisewski, B., Engbrodt, R., Gauger, S., Geibert, W., Geprägs, P., Gerdes, D., Gersonde, R., Gordon, A. L., Grobe, H., Hellmer, H. H., Isla, E., Jacobs, S. S., Janout, M., Jokat, W., Klages, M., Kuhn, G., Meincke, J., Ober, S., Østerhus, S., Peterson, R. G., Rabe, B., Rudels, B., Schauer, U., Schröder, M., Schumacher, S., Sieger, R., Sildam, J., Soltwedel, T., Stangeew, E., Stein, M., Strass, V. H., Thiede, J., Tippenhauer, S., Veth, C., von Appen, W.-J., Weirig, M.-F., Wisotzki, A., Wolf-Gladrow, D. A., and Kanzow, T.: From pole to pole: 33 years of physical oceanography onboard R/V Polarstern, *Earth Syst. Sci. Data*, 9, 211-220, <https://doi.org/10.5194/essd-9-211-2017>, 2017.

Fahrbach, E., Harms, S., Rohardt, G., Schröder, M., & Woodgate, R. A. (2001). Flow of bottom water in the northwestern Weddell Sea. *Journal of Geophysical Research: Oceans*, 106(C2), 2761-2778.

Fahrbach, E., Hoppema, M., Rohardt, G., Schröder, M., & Wisotzki, A. (2004). Decadal-scale variations of water mass properties in the deep Weddell Sea. *Ocean Dynamics*, 54(1), 77-91.

Fahrbach, E., Rohardt, G., and Sieger, R.: 25 Years of Polarstern hydrography (1982–2007), WDC-MARE Reports 5, Alfred-Wegener-Institut, Bremerhaven, 94 pp., 2007.

Fahrbach, E. and De Baar, H.: The Expedition of the Research Vessel Polarstern to the Antarctic in 2008 (ANT-XXIV/3). *Bericht zur Polar- und Meeresforschung*, Vol. 606, Alfred-Wegener-Institut, Bremerhaven, 228 pp., 2010.

Fahrbach, E., Hoppema, M., Rohardt, G., Boebel, O., Klatt, O., & Wisotzki, A. (2011). Warming of deep and abyssal water masses along the Greenwich meridian on decadal time scales: The Weddell gyre as a heat buffer. *Deep Sea Research Part II: Topical Studies in Oceanography*, 58(25), 2509-2523.

Ferreira, M. L., & Kerr, R. (2017). Source water distribution and quantification of North Atlantic Deep Water and Antarctic Bottom Water in the Atlantic Ocean. *Progress in Oceanography*, 153, 66-83.

- Foldvik, A., Gammelsrød, T., & Tørresen, T. (1985). Circulation and water masses on the southern Weddell Sea shelf. *Oceanology of the Antarctic continental shelf*, 5-20.
- Foster, T. D., & Carmack, E. C. (1976a). Frontal zone mixing and Antarctic Bottom Water formation in the southern Weddell Sea. *Deep Sea Research and Oceanographic Abstracts*. Vol. 23, No. 4, pp. 301-317
- Foster, T. D., & Carmack, E. C. (1976b). Temperature and salinity structure in the Weddell Sea. *Journal of Physical Oceanography*, 6(1), 36-44.
- Franco, B. C., Mata, M. M., Piola, A. R., & Garcia, C. A. (2007). Northwestern Weddell Sea deep outflow into the Scotia Sea during the austral summers of 2000 and 2001 estimated by inverse methods. *Deep Sea Research Part I: Oceanographic Research Papers*, 54(10), 1815-1840.
- Garcia-Ibanez, M. I., Pardo, P. C., Carracedo, L. I., Mercier, H., Lherminier, P., Rios, A. F., & Perez, F. F. (2015). Structure, transports and transformations of the water masses in the Atlantic Subpolar Gyre. *Progress in Oceanography*, 135, 18-36.
- Gill, A. E. (1973). Circulation and bottom water production in the Weddell Sea. *Deep Sea Research and Oceanographic Abstracts*. Vol. 20, No. 2, pp. 111-140.
- Gordon, A. L. (1978). Deep Antarctic convection west of Maud Rise. *Journal of Physical Oceanography*, 8(4), 600-612.
- Gordon, A. L. (2014). Oceanography: Southern Ocean polynya. *Nature Climate Change*, 4(4), 249-250.
- Gordon, A. L., Huber, B. A., Hellmer, H. H., & Field, A. (1993). Deep and bottom water of the Weddell Sea's western rim. *Science*, 262(5130), 95-98.
- Gordon, A. L., Visbeck, M., & Comiso, J. C. (2007). A possible link between the Weddell Polynya and the Southern Annular Mode. *Journal of Climate*, 20(11), 2558-2571.
- Gordon, A., Visbeck, M., & Huber, B. (2001). Export of Weddell Sea deep and bottom water. *Journal of Geophysical Research-Oceans*, 106, 9005-9017.
- Gouretski, V. V., & Danilov, A. I. (1993). Weddell Gyre: structure of the eastern boundary. *Deep Sea Research Part I: Oceanographic Research Papers*, 40(3), 561-582.
- Hellmer, H. H., Huhn, O., Gomis, D., & Timmermann, R. (2011). On the freshening of the northwestern Weddell Sea continental shelf. *Ocean Science*, 7(3), 305-316.
- Hellmer, H. H., Rhein, M., Heinemann, G., Abalichin, J., Abouchami, W., Baars, O., ... & Frank, M. (2016). Meteorology and oceanography of the Atlantic sector of the Southern Ocean—a review of German achievements from the last decade. *Ocean Dynamics*, 66(11), 1379-1413.

- Heywood, K. J., Naveira Garabato, A. C., & Stevens, D. P. (2002). High mixing rates in the abyssal Southern Ocean. *Nature*, 415(6875), 1011-1014.
- Heywood, K. J., Schmidtko, S., Heuzé, C., Kaiser, J., Jickells, T. D., Queste, B. Y., ... & Guihen, D. (2014). Ocean processes at the Antarctic continental slope. *Philosophical Transactions of the Royal Society of London A: Mathematical, Physical and Engineering Sciences*, 372(2019), 20130047.
- Huhn, O., Hellmer, H. H., Rhein, M., Rodehacke, C., Roether, W., Schodlok, M. P., & Schröder, M. (2008). Evidence of deep-and bottom-water formation in the western Weddell Sea. *Deep Sea Research Part II: Topical Studies in Oceanography*, 55(8), 1098-1116.
- Ivanov, V. V., Shapiro, G. I., Huthnance, J. M., Aleynik, D. L., & Golovin, P. N. (2004). Cascades of dense water around the world ocean. *Progress in oceanography*, 60(1), 47-98.
- Jackett, D. R., & McDougall, T. J. (1997). A neutral density variable for the world's oceans. *Journal of Physical Oceanography*, 27(2), 237-263.
- Jacobs, S. S. (2004). Bottom water production and its links with the thermohaline circulation. *Antarctic Science*, 16(04), 427-437.
- Jenkins, W. J., Smethie, W. M., Boyle, E. A., & Cutter, G. A. (2015). Water mass analysis for the US GEOTRACES (GA03) North Atlantic sections. *Deep Sea Research Part II: Topical Studies in Oceanography*, 116, 6-20.
- Johnson, G. C. (2008). Quantifying Antarctic bottom water and North Atlantic deep water volumes. *Journal of Geophysical Research: Oceans*, 113(C5).
- Johnson, D. R., Garcia, H. E., & Boyer, T. P. (2013). *World Ocean Database 2013 Tutorial*.
- Jullion, L., Jones, S. C., Naveira Garabato, A. C., & Meredith, M. P. (2010). Wind-controlled export of Antarctic Bottom Water from the Weddell Sea. *Geophysical Research Letters*, 37(9).
- Jullion, L., Naveira Garabato, A. C., Bacon, S., Meredith, M. P., Brown, P. J., Torres-Valdés, S., ... & Hoppema, M. (2014). The contribution of the Weddell Gyre to the lower limb of the Global Overturning Circulation. *Journal of Geophysical Research: Oceans*, 119(6), 3357-3377.
- Jullion, L., Naveira Garabato, A. C., Meredith, M. P., Holland, P. R., Courtois, P., & King, B. A. (2013). Decadal freshening of the Antarctic Bottom Water exported from the Weddell Sea. *Journal of Climate*, 26(20), 8111-8125.
- Karstensen, J., & Tomczak, M. (1997). Ventilation processes and water mass ages in the thermocline of the southeast Indian Ocean. *Geophysical Research Letters*, 24(22), 2777-2780.

- Karstensen, J., & Tomczak, M. (1998). Age determination of mixed water masses using CFC and oxygen data. *Journal of Geophysical Research: Oceans*, 103(C9), 18599-18609.
- Karstensen, J., & Tomczak, M. (1999). Manual for OMP Analysis Package for MATLAB, version 2.0.
- Kerr, R., Mata, M. M., & Garcia, C. A. (2009a). On the temporal variability of the Weddell Sea Deep Water masses. *Antarctic Science*, 21(4), 383.
- Kerr, R., Wainer, I., & Mata, M. M. (2009b). Representation of the Weddell Sea deep water masses in the ocean component of the NCAR-CCSM model. *Antarctic Science*, 21(03), 301-312.
- Kerr, R., K. J. Heywood, M. M. Mata, and C. A. E. Garcia (2012a), On the outflow of dense water from the Weddell and Ross Seas in OCCAM model, *Ocean Sci.*, 8(3), 369–388, doi:10.5194/os-8-369-2012.
- Kerr, R., Wainer, I. L. A. N. A., Mata, M. M., & Garcia, C. A. (2012b). Quantifying Antarctic deep waters in SODA reanalysis product. *Pesquisa Antártica Brasileira*, 5, 47-59.
- Kitade, Y., Shimada, K., Tamura, T., Williams, G. D., Aoki, S., Fukamachi, Y., ... & Ohshima, K. I. (2014). Antarctic bottom water production from the Vincennes Bay polynya, East Antarctica. *Geophysical Research Letters*, 41(10), 3528-3534.
- Klatt, O., Fahrbach, E., Hoppema, M., & Rohardt, G. (2005). The transport of the Weddell Gyre across the Prime Meridian. *Deep Sea Research Part II: Topical Studies in Oceanography*, 52(3), 513-528.
- Leach, H., Strass, V., & Cisewski, B. (2011). Modification by lateral mixing of the Warm Deep Water entering the Weddell Sea in the Maud Rise region. *Ocean Dynamics*, 61(1), 51-68.
- Leffanue, H., & Tomczak, M. (2004). Using OMP analysis to observe temporal variability in water mass distribution. *Journal of Marine Systems*, 48(1), 3-14.
- Mackas, D. L., Denman, K. L., & Bennett, A. F. (1987). Least squares multiple tracer analysis of water mass composition. *Journal of Geophysical Research: Oceans*, 92(C3), 2907-2918.
- Mamayev, O.I., 1975. *Temperature-Salinity Analysis of World Ocean Waters*. Elsevier, Amsterdam.
- Meredith, M. P. (2016). Understanding the structure of changes in the Southern Ocean eddy field. *Geophysical Research Letters*, 43(11), 5829-5832.
- Meredith, M. P., Gordon, A. L., Naveira Garabato, A. C., Abrahamsen, E. P., Huber, B. A., Jullion, L., & Venables, H. J. (2011). Synchronous intensification and warming of Antarctic Bottom Water outflow from the Weddell Gyre. *Geophysical Research Letters*, 38(3).

- Meredith, M. P., Heywood, K. J., Frew, R. D., & Dennis, P. F. (1999). Formation and circulation of the water masses between the southern Indian Ocean and Antarctica: Results from 18O. *Journal of marine research*, 57(3), 449-470.
- Meredith, M. P., Jullion, L., Brown, P. J., Garabato, A. C. N., & Couldrey, M. P. (2014). Dense waters of the Weddell and Scotia Seas: recent changes in properties and circulation. *Philosophical Transactions of the Royal Society of London A: Mathematical, Physical and Engineering Sciences*, 372(2019), 20130041.
- Meredith, M. P., Locarnini, R. A., Van Scoy, K. A., Watson, A. J., Heywood, K. J., & King, B. A. (2000). On the sources of Weddell Gyre Antarctic bottom water. *Journal of Geophysical Research: Oceans*, 105(C1), 1093-1104.
- Meredith, M. P., Mazloff, M., Sallée, J. B., Newman, L., Wahlin, A., Williams, M. J. M., ... & Schmidt, S. (2015). The Southern Ocean Observing System (SOOS). *Bulletin of the American Meteorological Society*, 96(7), S157-S160.
- Meredith, M. P., Naveira Garabato, A. C. N., Gordon, A. L., & Johnson, G. C. (2008). Evolution of the deep and bottom waters of the Scotia Sea, Southern Ocean, during 1995–2005. *Journal of Climate*, 21(13), 3327-3343.
- Meredith, M. P., Schofield, O., Newman, L., Urban, E., & Sparrow, M. (2013). The vision for a Southern Ocean observing system. *Current Opinion in Environmental Sustainability*, 5(3), 306-313.
- Muench, R.D.; Hellmer, H. H. (2002). The international DOVETAIL program. *Deep Sea Research Part II: Topical Studies in Oceanography*
- Naveira Garabato, A. C., McDonagh, E. L., Stevens, D. P., Heywood, K. J., & Sanders, R. J. (2002). On the export of Antarctic bottom water from the Weddell Sea. *Deep Sea Research Part II: Topical Studies in Oceanography*, 49(21), 4715-4742.
- Naveira Garabato, A. C., Williams, A. P., & Bacon, S. (2014). The three-dimensional overturning circulation of the Southern Ocean during the WOCE era. *Progress in Oceanography*, 120, 41-78.
- Nicholls, K. W., Østerhus, S., Makinson, K., & Johnson, M. R. (2001). Oceanographic conditions south of Berkner Island, beneath Filchner- Ronne Ice Shelf, Antarctica. *Journal of Geophysical Research: Oceans*, 106(C6), 11481-11492.
- Foldvik, A., Gammelsrød, T., Østerhus, S., Fahrbach, E., Rohardt, G., Schröder, M., ... & Woodgate, R. A. (2004). Ice shelf water overflow and bottom water formation in the southern Weddell Sea. *Journal of Geophysical Research: Oceans*, 109(C2).
- Nicholls, K. W., Østerhus, S., Makinson, K., Gammelsrød, T., & Fahrbach, E. (2009). Ice-ocean processes over the continental shelf of the southern Weddell Sea, Antarctica: A review. *Reviews of Geophysics*, 47(3).

- Orsi, A. H., Jacobs, S. S., Gordon, A. L., & Visbeck, M. (2001). Cooling and ventilating the abyssal ocean. *Geophysical Research Letters*, 28(15), 2923-2926.
- Orsi, A. H., Johnson, G. C., & Bullister, J. L. (1999). Circulation, mixing, and production of Antarctic Bottom Water. *Progress in Oceanography*, 43(1), 55-109.
- Orsi, A. H., Smethie, W. M., & Bullister, J. L. (2002). On the total input of Antarctic waters to the deep ocean: A preliminary estimate from chlorofluorocarbon measurements. *Journal of Geophysical Research: Oceans*, 107(C8).
- Ohshima, K. I., Fukamachi, Y., Williams, G. D., Nihashi, S., Roquet, F., Kitade, Y., ... & Hindell, M. (2013). Antarctic Bottom Water production by intense sea-ice formation in the Cape Darnley polynya. *Nature Geoscience*, 6(3), 235-240.
- Pardo, P. C., Pérez, F. F., Velo, A., & Gilcoto, M. (2012). Water masses distribution in the Southern Ocean: Improvement of an extended OMP (eOMP) analysis. *Progress in Oceanography*, 103, 92-105.
- Pritchard, H. D., & Vaughan, D. G. (2007). Widespread acceleration of tidewater glaciers on the Antarctic Peninsula. *Journal of Geophysical Research: Earth Surface*, 112(F3).
- Purkey, S. G., & Johnson, G. C. (2010). Warming of global abyssal and deep Southern Ocean waters between the 1990s and 2000s: Contributions to global heat and sea level rise budgets. *Journal of Climate*, 23(23), 6336-6351.
- Purkey, S. G., & Johnson, G. C. (2012). Global contraction of Antarctic Bottom Water between the 1980s and 2000s. *Journal of Climate*, 25(17), 5830-5844.
- Purkey, S. G., & Johnson, G. C. (2013). Antarctic Bottom Water warming and freshening: Contributions to sea level rise, ocean freshwater budgets, and global heat gain. *Journal of Climate*, 26(16), 6105-6122.
- Poole, R., & Tomczak, M. (1999). Optimum multiparameter analysis of the water mass structure in the Atlantic Ocean thermocline. *Deep Sea Research Part I: Oceanographic Research Papers*, 46(11), 1895-1921.
- Rignot, E., Bamber, J. L., Van Den Broeke, M. R., Davis, C., Li, Y., Van De Berg, W. J., & Van Meijgaard, E. (2008). Recent Antarctic ice mass loss from radar interferometry and regional climate modelling. *Nature Geoscience*, 1(2), 106-110.
- Rintoul, S. R. (2007). Rapid freshening of Antarctic Bottom Water formed in the Indian and Pacific oceans. *Geophysical Research Letters*, 34(6).
- Rohardt, G., Fahrbach, E., and Wisotzki, A.: Physical oceanography during POLARSTERN cruise ANT-XXVII/2, Alfred Wegener Institute, Helmholtz Center for Polar and Marine Research, Bremerhaven, doi:10.1594/PANGAEA.772244, 2011.

- Rohardt, Gerd; Boebel, Olaf (2015): Physical oceanography during POLARSTERN cruise PS89 (ANT-XXX/2). Alfred Wegener Institute, Helmholtz Center for Polar and Marine Research, Bremerhaven, doi:10.1594/PANGAEA.846701.
- Ryan, S., Schröder, M., Huhn, O., & Timmermann, R. (2016). On the warm inflow at the eastern boundary of the Weddell Gyre. *Deep Sea Research Part I: Oceanographic Research Papers*, 107, 70-81.
- Robertson, R., Visbeck, M., Gordon, A. L., & Fahrbach, E. (2002). Long-term temperature trends in the deep waters of the Weddell Sea. *Deep Sea Research Part II: Topical Studies in Oceanography*, 49(21), 4791-4806.
- Santos, G. C., Kerr, R., Azevedo, J. L. L., Mendes, C. R. B., & da Cunha, L. C. (2016). Influence of Antarctic Intermediate Water on the deoxygenation of the Atlantic Ocean. *Dynamics of Atmospheres and Oceans*, 76, 72-82.
- Schmidtke, S., Heywood, K. J., Thompson, A. F., & Aoki, S. (2014). Multidecadal warming of Antarctic waters. *Science*, 346(6214), 1227-1231.
- Sloyan, B. M. (2005). Spatial variability of mixing in the Southern Ocean. *Geophysical research letters*, 32(18).
- Sokolov, S., & Rintoul, S. R. (2009). Circumpolar structure and distribution of the Antarctic Circumpolar Current fronts: 2. Variability and relationship to sea surface height. *Journal of Geophysical Research: Oceans*, 114(C11).
- Schröder, M., & Fahrbach, E. (1999). On the structure and the transport of the eastern Weddell Gyre. *Deep Sea Research Part II: Topical Studies in Oceanography*, 46(1), 501-527.
- Schröder, M., Hellmer, H. H., & Absy, J. M. (2002). On the near-bottom variability in the northwestern Weddell Sea. *Deep Sea Research Part II: Topical Studies in Oceanography*, 49(21), 4767-4790.
- Talley, L. D. (2013). Closure of the global overturning circulation through the Indian, Pacific, and Southern Oceans: Schematics and transports. *Oceanography*, 26(1), 80-97.
- Tomczak, M. (1981). A multi-parameter extension of temperature/salinity diagram techniques for the analysis of non-isopycnal mixing. *Progress in Oceanography*, 10(3), 147-171.
- Tomczak, M. (1999). Some historical, theoretical and applied aspects of quantitative water mass analysis. *Journal of Marine Research*, 57(2), 275-303.
- Tomczak, M., & Large, D. G. (1989). Optimum multiparameter analysis of mixing in the thermocline of the eastern Indian Ocean. *Journal of Geophysical Research: Oceans*, 94(C11), 16141-16149.
- Tomczak, M., & Liefink, S. (2005). Interannual variations of water mass volumes in the Southern Ocean. *Journal of Atmospheric & Ocean Science*, 10(1), 31-42.

- van Caspel, M., Schröder, M., Huhn, O., & Hellmer, H. H. (2015). Precursors of Antarctic Bottom Water formed on the continental shelf off Larsen Ice Shelf. *Deep Sea Research Part I: Oceanographic Research Papers*, 99, 1-9.
- van Heuven, S. M., Hoppema, M., Huhn, O., Slagter, H. A., & de Baar, H. J. (2011). Direct observation of increasing CO₂ in the Weddell Gyre along the Prime Meridian during 1973–2008. *Deep Sea Research Part II: Topical Studies in Oceanography*, 58(25), 2613-2635.
- van Heuven, S. M., Hoppema, M., Jones, E. M., & de Baar, H. J. (2014). Rapid invasion of anthropogenic CO₂ into the deep circulation of the Weddell Gyre. *Phil. Trans. R. Soc. A*, 372(2019), 20130056.
- van Sebille, E., Spence, P., Mazloff, M. R., England, M. H., Rintoul, S. R., & Saenko, O. A. (2013). Abyssal connections of Antarctic Bottom Water in a Southern Ocean state estimate. *Geophysical Research Letters*, 40(10), 2177-2182.
- von Gyldenfeldt, A. B., Fahrbach, E., García, M. A., & Schröder, M. (2002). Flow variability at the tip of the Antarctic Peninsula. *Deep Sea Research Part II: Topical Studies in Oceanography*, 49(21), 4743-4766.
- Whitworth, T., & Nowlin, W. D. (1987). Water masses and currents of the Southern Ocean at the Greenwich Meridian. *Journal of Geophysical Research: Oceans*, 92(C6), 6462-6476.
- Whitworth, T., III, A. H. Orsi, S.-J. Kim, and W. D. Nowlin Jr., 1998. Water masses and mixing near the Antarctic Slope Front. *Ocean, Ice, and Atmosphere: Interactions at the Antarctic Continental Margin*, S. S. Jacobs and R. F. Weiss, Eds., Antarctic Research Series, Amer. Geophys. Union, 1–27.
- Wijk, E. M., & Rintoul, S. R. (2014). Freshening drives contraction of Antarctic bottom water in the Australian Antarctic Basin. *Geophysical Research Letters*, 41(5), 1657-1664.